Response of a Fabry-Perot optical trap to a gravitational wave:

The case for fully relativistic detector analyses

Andrew Laeuger (Caltech), Nancy Aggarwal (University of California, Davis), and the LSD Collaboration (Northwestern University, Clarkson University)

Optomechanical Sensing for Subatomic and Astroparticle Physics, Kingston, ON, Canada, Sep 2026

Levitated sensors for high frequency GW detection

- Levitated sensors are a promising platform for searches for high frequency GWs
  - GW displaces the optical trap site, inducing driving force on sensor

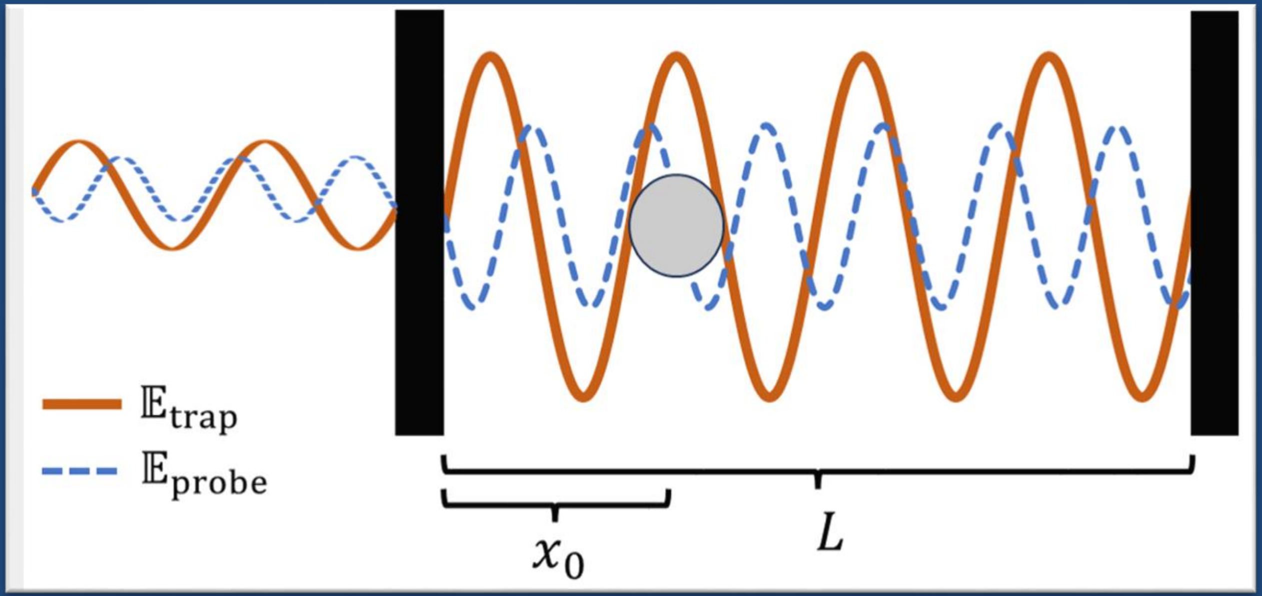

Levitated sensors for high frequency GW detection

- Levitated sensors are a promising platform for searches for high frequency GWs
  - GW displaces the optical trap site, inducing driving force on sensor
  - Inherently narrowband detection concept, but the band can be scanned
    - A few tens to hundreds of kHz is possible by varying sensor mass, laser power

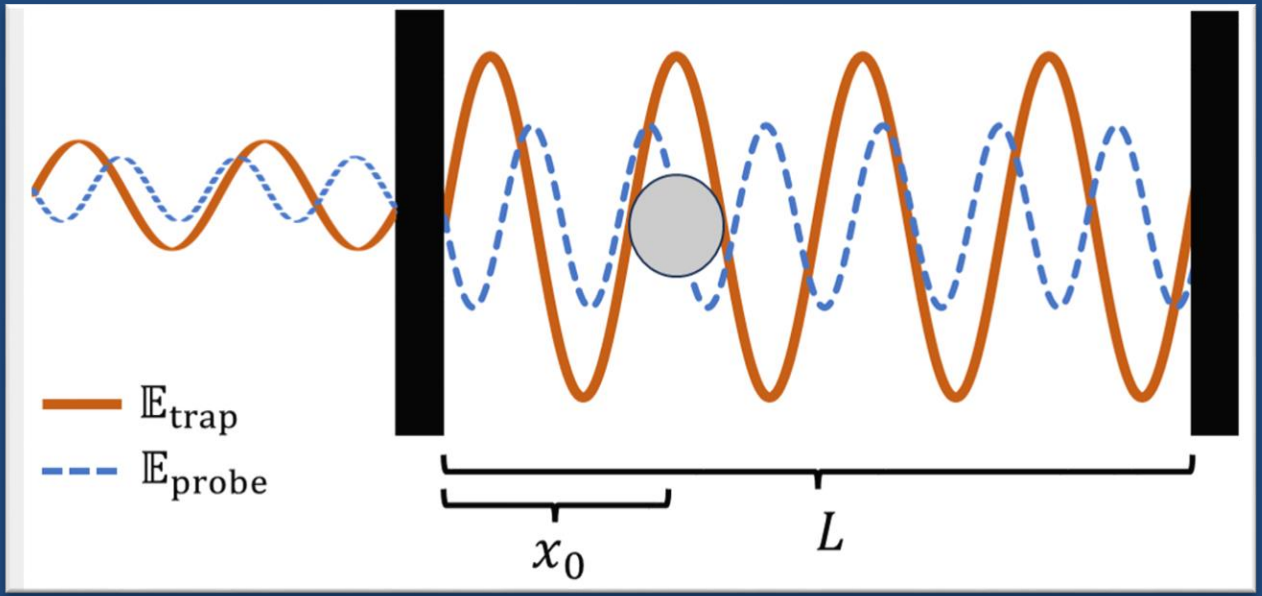

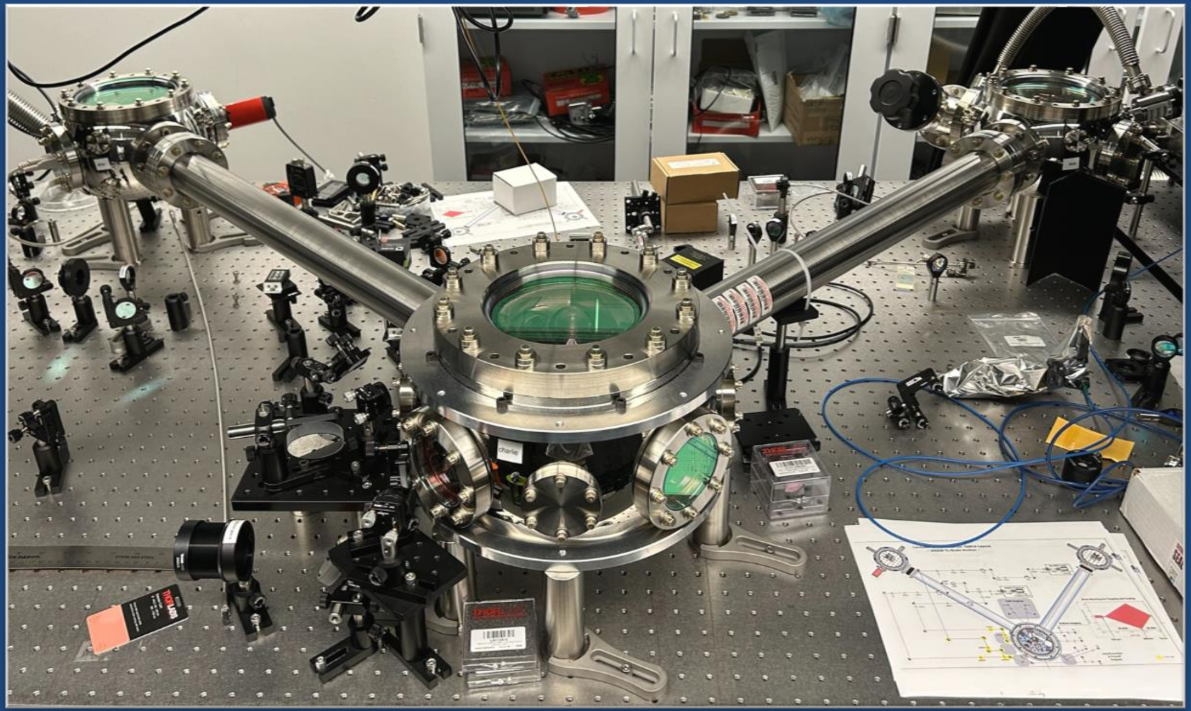

Relativistic response in small particle limit

- How can we derive the GW-induced displacement of the trap potential minimum relative to a levitated sensor?

arXiv:2603.07302

Relativistic response in small particle limit

- How can we derive the GW-induced displacement of the trap potential minimum relative to a levitated sensor?

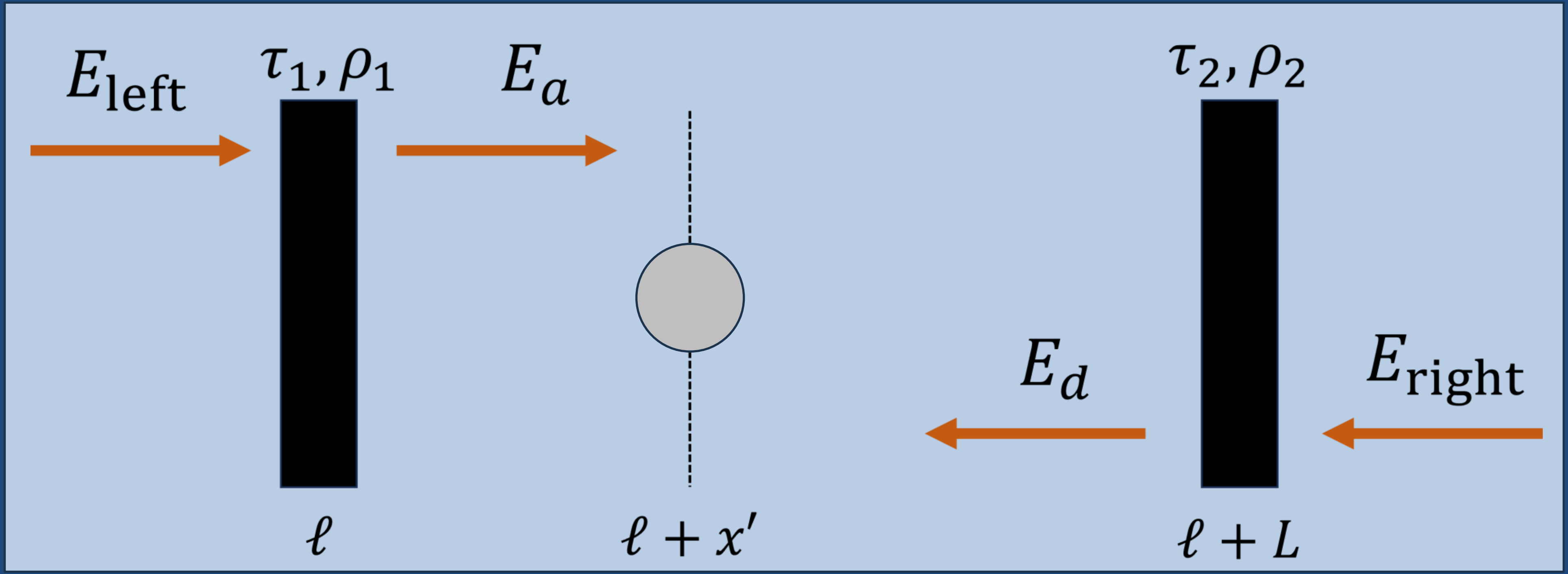

arXiv:2603.07302

Relativistic response in small particle limit

- How can we derive the GW-induced displacement of the trap potential minimum relative to a levitated sensor?

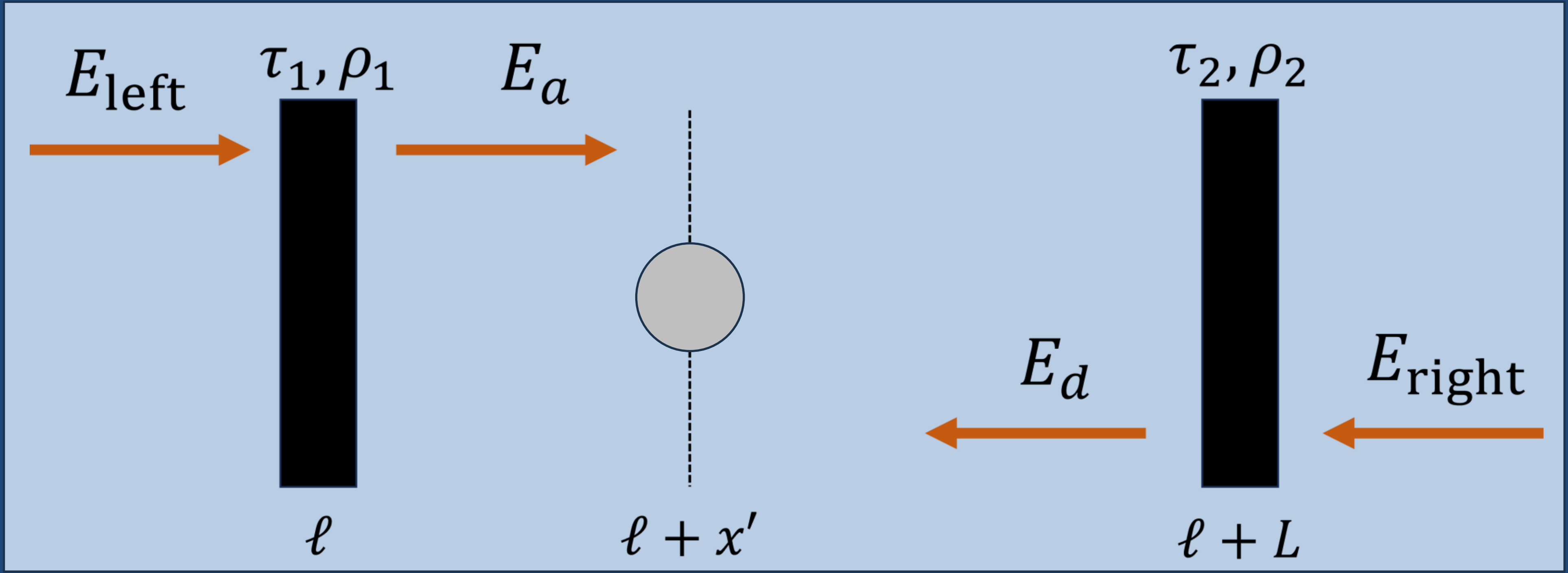

$$E_a(t) = \tau_1 E_{\text{left}}(t) - \rho_1 E_d(t - T(\ell + L, \ell)[t]),$$

arXiv:2603.07302

Relativistic response in small particle limit

- How can we derive the GW-induced displacement of the trap potential minimum relative to a levitated sensor?

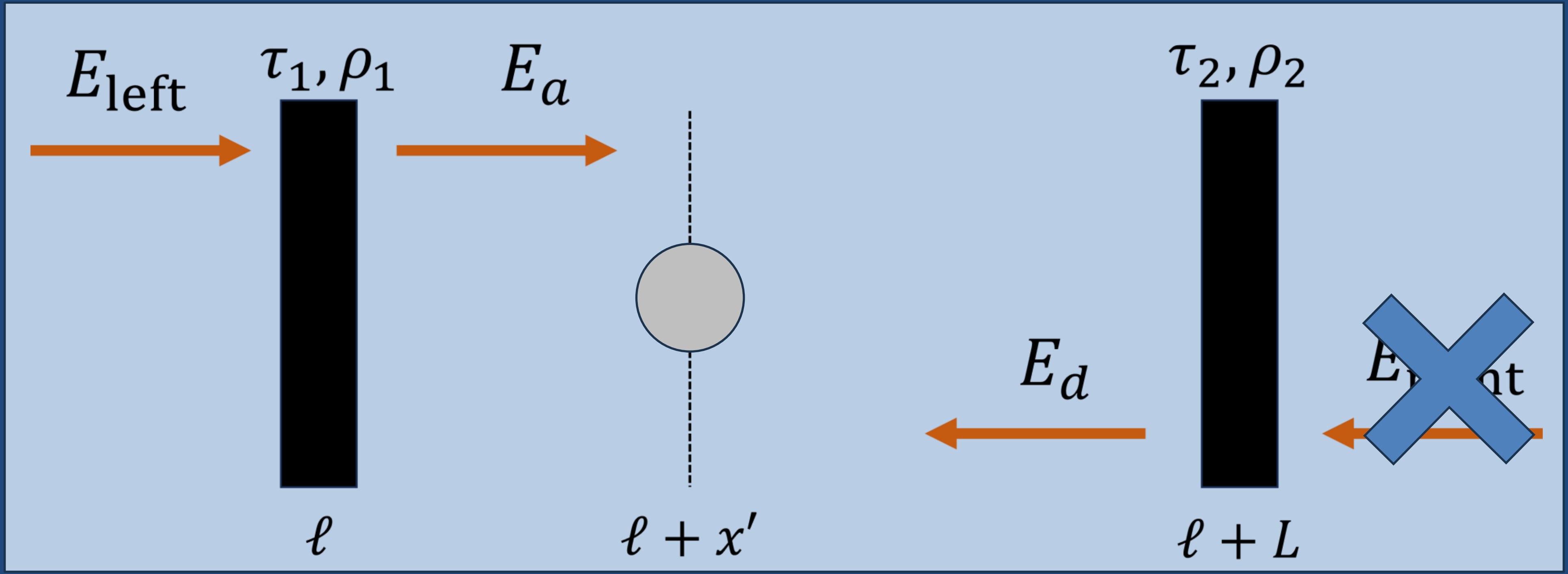

$$E_a(t) = \tau_1 E_{\text{left}}(t) - \rho_1 E_d(t - T(\ell + L, \ell)[t]),$$

$$E_d(t) = -\rho_2 E_a(t - T(\ell, \ell + L)[t]),$$

arXiv:2603.07302

Relativistic response in small particle limit

$$E_a(t) = \tau_1 \sum_{n=0}^{\infty} (\rho_1 \rho_2)^n E_{\text{left}}(t - \sum_{j=0}^{n} T_j)$$

$$\begin{aligned}
T_0 &= 0, \\
T_1 &= T(\ell + L, \ell)[t] + T(\ell, \ell + L)\left[t - T(\ell + L, \ell)[t]\right], \\
T_2 &= T(\ell + L, \ell)[t - T_1] \\
&\quad + T(\ell, \ell + L)\left[t - T_1 - T(\ell + L, \ell)[t - T_1]\right],
\end{aligned}$$

(outbound and return trips in cavity)

Relativistic response in small particle limit

$$E_a(t) = \tau_1 \sum_{n=0}^{\infty} (\rho_1 \rho_2)^n E_{\text{left}}(t - \sum_{j=0}^{n} T_j)$$

$$\begin{aligned} T_0 &= 0, \\ T_1 &= T(\ell + L, \ell)[t] + T(\ell, \ell + L)\big[t - T(\ell + L, \ell)[t]\big], \\ T_2 &= T(\ell + L, \ell)[t - T_1] \\ &\quad + T(\ell, \ell + L)\big[t - T_1 - T(\ell + L, \ell)[t - T_1]\big], \end{aligned}$$

(outbound and return trips in cavity)

No GW → $T_1, T_2, \ldots = 2L/c$

Relativistic response in small particle limit

$$E_a(t) = \tau_1 \sum_{n=0}^{\infty} (\rho_1 \rho_2)^n E_{\text{left}}(t - \sum_{j=0}^{n} T_j)$$

$$\begin{aligned}
T_0 &= 0, \\
T_1 &= T(\ell + L, \ell)[t] + T(\ell, \ell + L)\big[t - T(\ell + L, \ell)[t]\big], \\
T_2 &= T(\ell + L, \ell)[t - T_1] \\
&\quad + T(\ell, \ell + L)\big[t - T_1 - T(\ell + L, \ell)[t - T_1]\big],
\end{aligned}$$

(outbound and return trips in cavity)

Transverse-Traceless (TT) Gauge

- Free masses stay at fixed comoving coordinates, distances change through metric

Relativistic response in small particle limit

$$E_a(t) = \tau_1 \sum_{n=0}^{\infty} (\rho_1 \rho_2)^n E_{\text{left}}(t - \sum_{j=0}^{n} T_j)$$

$$\begin{aligned} T_0 &= 0, \\ T_1 &= T(\ell + L, \ell)[t] + T(\ell, \ell + L)\big[t - T(\ell + L, \ell)[t]\big], \\ T_2 &= T(\ell + L, \ell)[t - T_1] \\ &\quad + T(\ell, \ell + L)\big[t - T_1 - T(\ell + L, \ell)[t - T_1]\big], \end{aligned}$$

(outbound and return trips in cavity)

Transverse-Traceless (TT) Gauge

- Free masses stay at fixed comoving coordinates, distances change through metric
- Modified coordinate velocity of light

$$-c^2 \frac{d^2 t}{d\xi^2} + \big(1 + h(t)\big) \frac{d^2 x}{d\xi^2} = 0$$

$$\rightarrow \frac{dt}{dx} \approx \frac{1}{c}\left(1 + \frac{h(t)}{2}\right)$$

Relativistic response in small particle limit

$$E_a(t) = \tau_1 \sum_{n=0}^{\infty} (\rho_1\rho_2)^n E_{\text{left}}\left(t - \sum_{j=0}^{n} T_j\right)$$

$$\begin{aligned}
T_0 &= 0, \\
T_1 &= T(\ell+L,\ell)[t] + T(\ell,\ell+L)\big[t - T(\ell+L,\ell)[t]\big], \\
T_2 &= T(\ell+L,\ell)[t-T_1] \\
&\quad + T(\ell,\ell+L)\big[t - T_1 - T(\ell+L,\ell)[t-T_1]\big],
\end{aligned}$$

(outbound and return trips in cavity)

Transverse-Traceless (TT) Gauge

- Free masses stay at fixed comoving coordinates, distances change through metric
- Modified coordinate velocity of light

$$-c^2\frac{d^2t}{d\xi^2} + \big(1+h(t)\big)\frac{d^2x}{d\xi^2} = 0$$

$$\rightarrow \frac{dt}{dx} \approx \frac{1}{c}\left(1 + \frac{h(t)}{2}\right)$$

Local Lorentz (LL) Gauge

- Now, free masses move the familiar $x \rightarrow x(1+h(t)/2)$ while coordinates remain fixed

Relativistic response in small particle limit

$$E_a(t) = \tau_1 \sum_{n=0}^{\infty} (\rho_1 \rho_2)^n E_{\text{left}}(t - \sum_{j=0}^{n} T_j)$$

$$\begin{aligned} T_0 &= 0, \\ T_1 &= T(\ell + L, \ell)[t] + T(\ell, \ell + L)\big[t - T(\ell + L, \ell)[t]\big], \\ T_2 &= T(\ell + L, \ell)[t - T_1] \\ &\quad + T(\ell, \ell + L)\big[t - T_1 - T(\ell + L, \ell)[t - T_1]\big], \end{aligned}$$

(outbound and return trips in cavity)

Transverse-Traceless (TT) Gauge

- Free masses stay at fixed comoving coordinates, distances change through metric
- Modified coordinate velocity of light

$$-c^2 \frac{d^2 t}{d\xi^2} + \big(1 + h(t)\big) \frac{d^2 x}{d\xi^2} = 0$$

$$\rightarrow \frac{dt}{dx} \approx \frac{1}{c}\left(1 + \frac{h(t)}{2}\right)$$

Local Lorentz (LL) Gauge

- Now, free masses move the familiar $x \rightarrow x(1 + h(t)/2)$ while coordinates remain fixed
- Beyond lowest order, photon coordinate velocity is modified again
- Furthermore, GW changes the clock ticking rate at fixed coordinates

Relativistic response in small particle limit

$$E_a(t) = \tau_1 \sum_{n=0}^{\infty} (\rho_1\rho_2)^n E_{\mathrm{left}}\left(t - \sum_{j=0}^{n} T_j\right)$$

$$\begin{aligned} T_0 &= 0, \\ T_1 &= T(\ell+L,\ell)[t] + T(\ell,\ell+L)\big[t - T(\ell+L,\ell)[t]\big], \\ T_2 &= T(\ell+L,\ell)[t - T_1] \\ &\quad + T(\ell,\ell+L)\big[t - T_1 - T(\ell+L,\ell)[t - T_1]\big], \end{aligned}$$

(outbound and return trips in cavity)

Transverse-Traceless (TT) Gauge

- Free masses stay at fixed comoving coordinates, distances change through metric
- Modified coordinate velocity of light

$$-c^2 \frac{d^2 t}{d\xi^2} + \big(1 + h(t)\big)\frac{d^2 x}{d\xi^2} = 0$$

$$\rightarrow \frac{dt}{dx} \approx \frac{1}{c}\left(1 + \frac{h(t)}{2}\right)$$

Local Lorentz (LL) Gauge

- Now, free masses move the familiar $x \rightarrow x(1 + h(t)/2)$ while coordinates remain fixed
- Beyond lowest order, photon coordinate velocity is modified again
- Furthermore, GW changes the clock ticking rate at fixed coordinates

→ Much more algebraically complex than TT Gauge

Relativistic response in small particle limit

- The ***gauge-invariant*** relative displacement between levitated sensor and the antinode it sits at for $h(t) = h_0 \cos(\Omega t)$ is:

$\mathcal{O}(\Omega L/c)$ correction $\sim \mathcal{F}$

$$h_0(L - x_0)/2 \times \left(\cos(\Omega t) - \frac{\Omega L}{c} \frac{|r^2 - 1|}{|r - 1|^2} \sin(\Omega t) \right)$$

arXiv:2603.07302

Relativistic response in small particle limit

- The *gauge-invariant* relative displacement between levitated sensor and the antinode it sits at for $h(t) = h_0\cos(\Omega t)$ is:

$\mathcal{O}(\Omega L/c)$ correction $\sim \mathcal{F}$

$$h_0(L - x_0)/2 \times \left(\cos(\Omega t) - \frac{\Omega L}{c}\frac{|r^2 - 1|}{|r - 1|^2}\sin(\Omega t)\right)$$

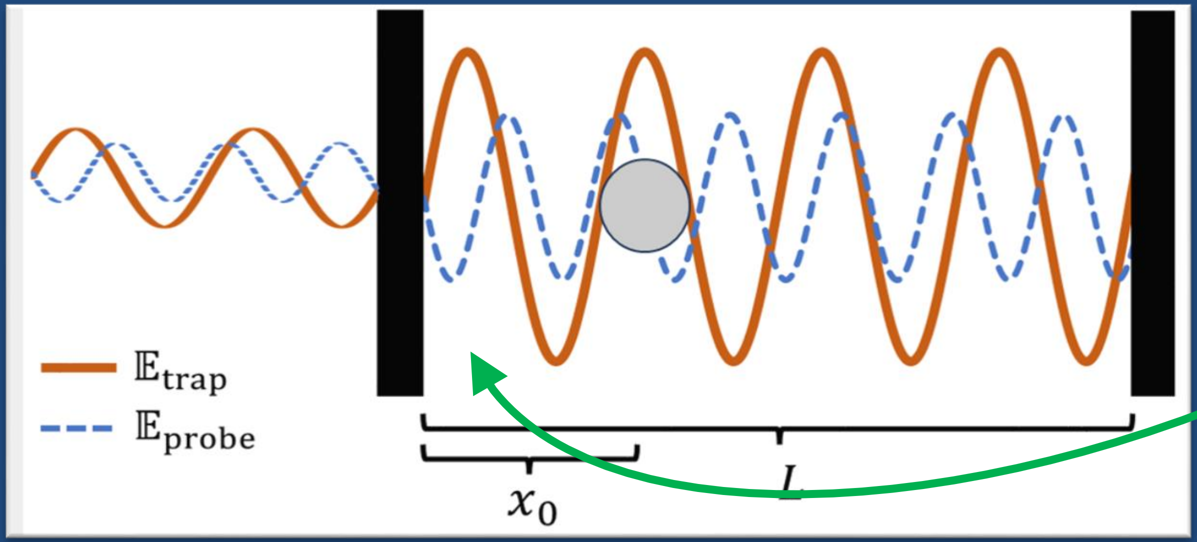

Ideally want sensor levitated as close to the input mirror as possible!

arXiv:2603.07302

Input/End-mirror asymmetry and consequences

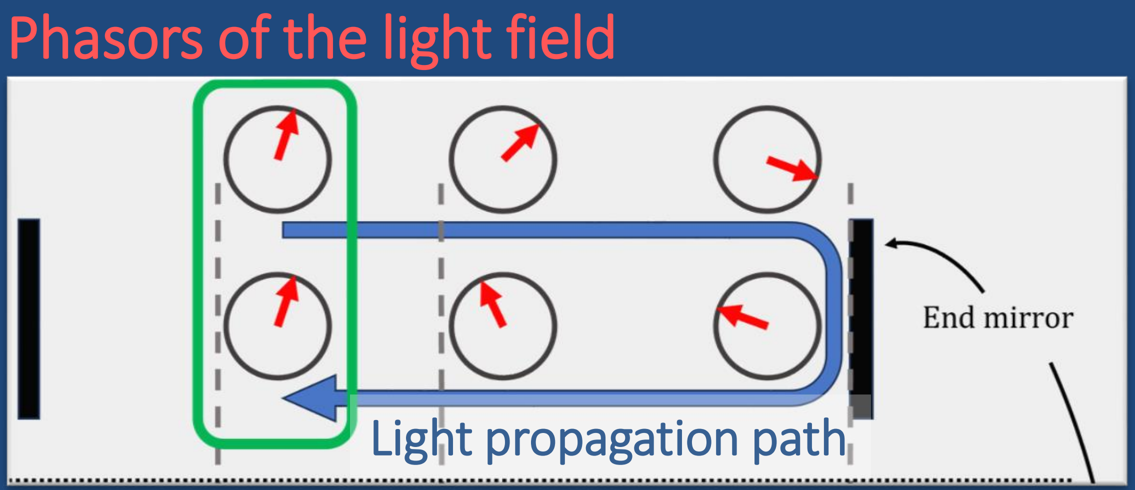

arXiv:2603.07302

Input/End-mirror asymmetry and consequences

- Antinodes appear where counterpropagating waves are in phase
- Phase offset is simple for end mirror reflection

Phasors of the light field

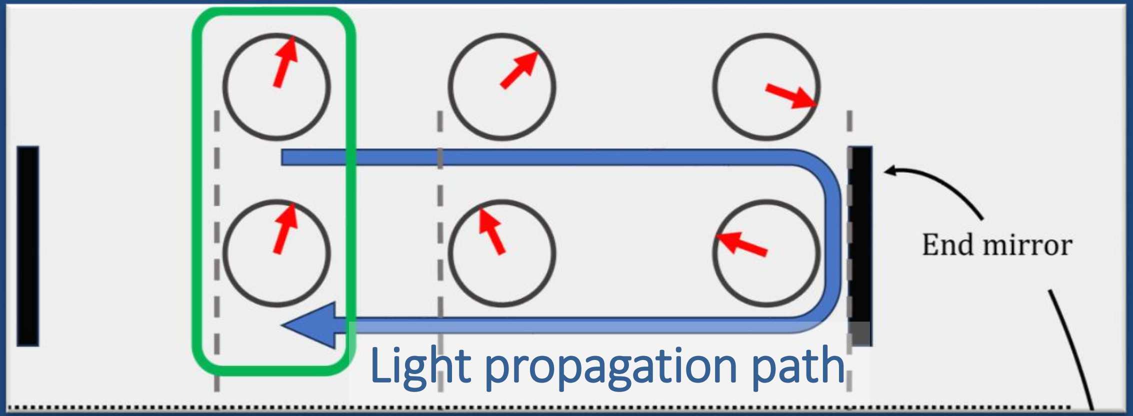

arXiv:2603.07302

Input/End-mirror asymmetry and consequences

- Antinodes appear where counterpropagating waves are in phase
- Phase offset is simple for end mirror reflection
  - In slow motion limit, end mirror is the exact midpoint → antinodes anchored to end mirror

Phasors of the light field

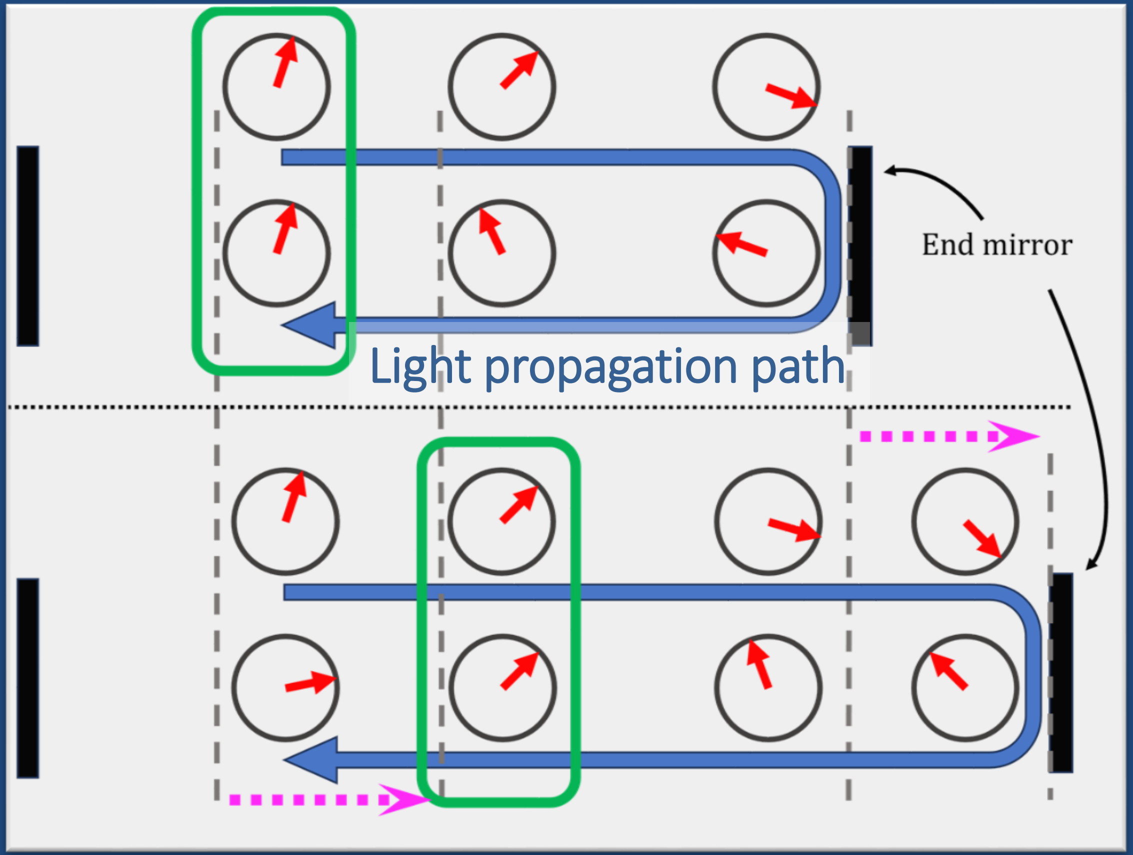

arXiv:2603.07302

Input/End-mirror asymmetry and consequences

- Antinodes appear where counterpropagating waves are in phase
- Phase offset is simple for end mirror reflection
  - In slow motion limit, end mirror is the exact midpoint → antinodes anchored to end mirror
- In the LL gauge, the mirror moves by $h(t)(\ell + L)/2$; all antinodes move same amount
  - Indeed, $\delta x^{\mathrm{LL}}_{\mathrm{antinode}} \approx h_0(\ell + L)/2 \times \cos \Omega t$

Phasors of the light field

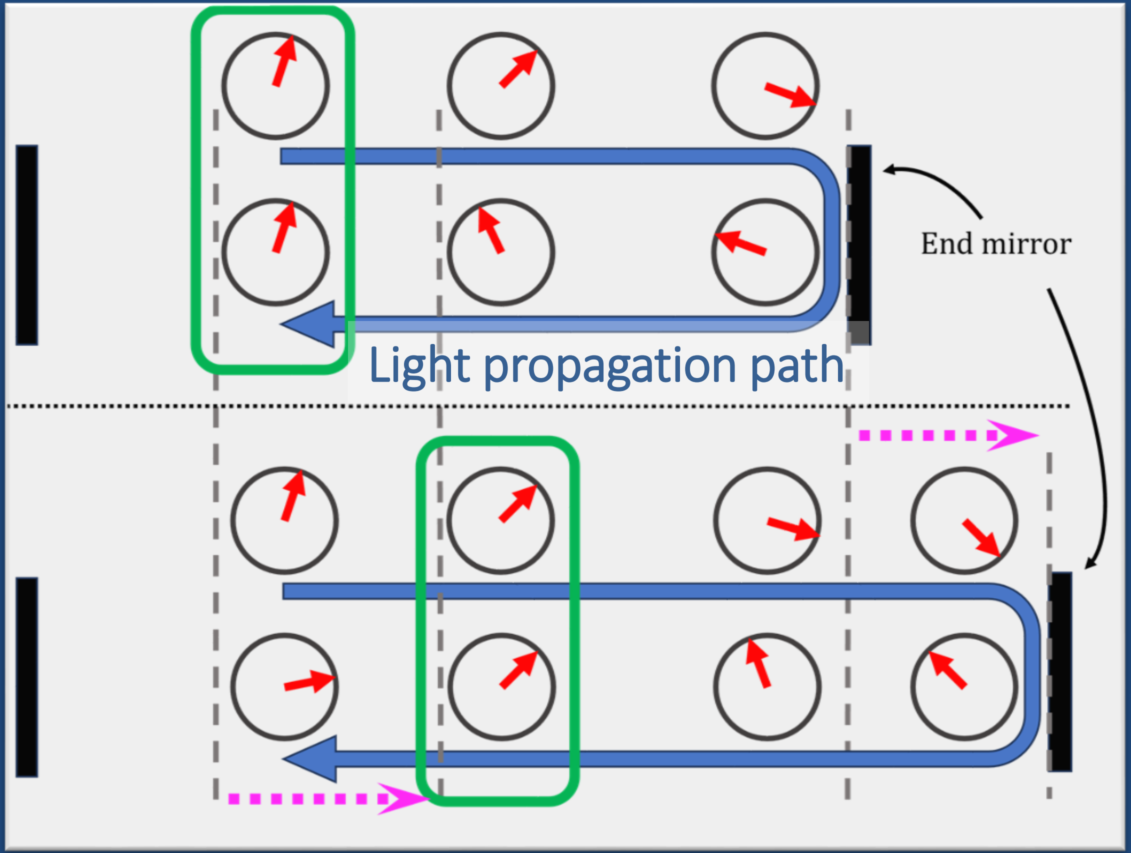

arXiv:2603.07302

Input/End-mirror asymmetry and consequences

- Antinodes appear where counterpropagating waves are in phase
- Phase offset is simple for end mirror reflection
  - In slow motion limit, end mirror is the exact midpoint → antinodes anchored to end mirror
- In the LL gauge, the mirror moves by $h(t)(\ell + L)/2$; all antinodes move same amount
  - Indeed, $\delta x^{\mathrm{LL}}_{\mathrm{antinode}} \approx h_0(\ell + L)/2 \times \cos\Omega t$
  - Sensor moves by $h_0(\ell + x_0)/2 \times \cos\Omega t$, yielding the asymmetry

Phasors of the light field

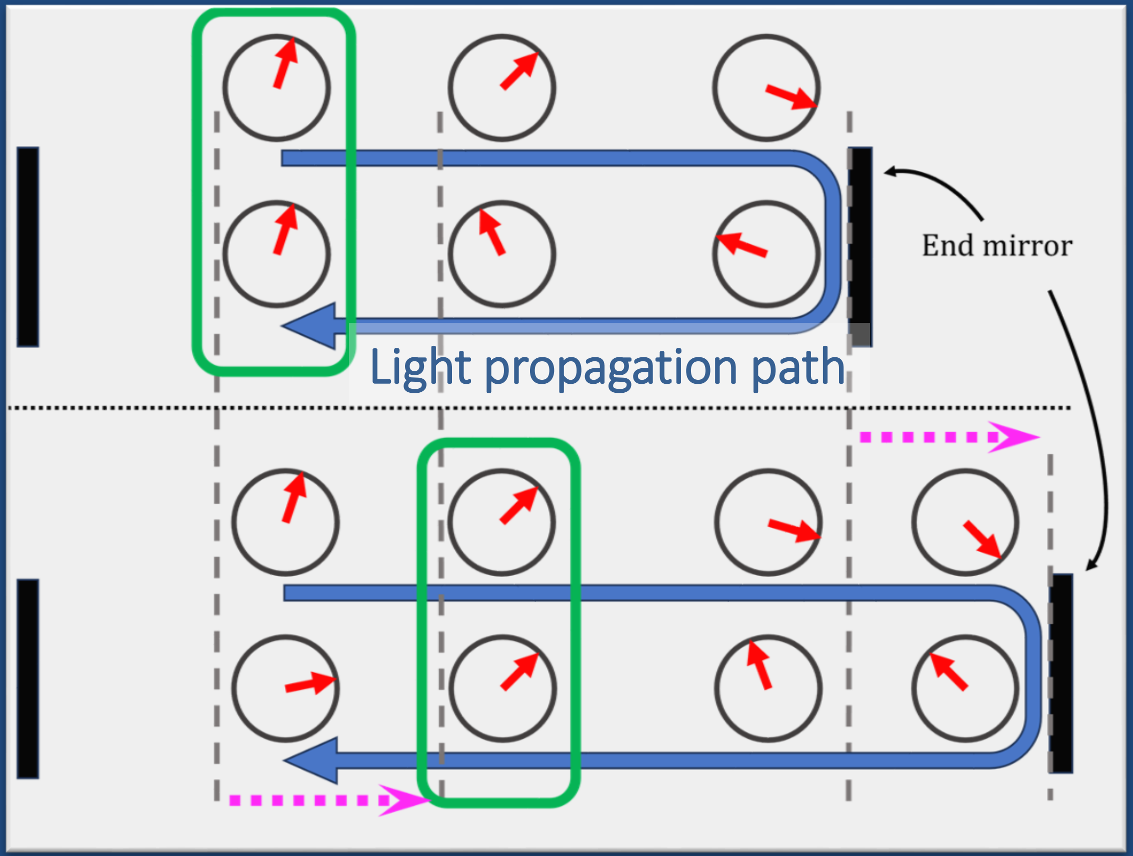

arXiv:2603.07302

Input/End-mirror asymmetry and consequences

- Antinodes appear where counterpropagating waves are in phase
- Phase offset is simple for end mirror reflection
  - In slow motion limit, end mirror is the exact midpoint → antinodes anchored to end mirror
- In the LL gauge, the mirror moves by $h(t)(\ell + L)/2$; all antinodes move same amount
  - Indeed, $\delta x^{\mathrm{LL}}_{\mathrm{antinode}} \approx h_0(\ell + L)/2 \times \cos\Omega t$
  - Sensor moves by $h_0(\ell + x_0)/2 \times \cos\Omega t$, yielding the asymmetry
- In TT gauge, the phasors rotate faster in space
  - Antinodes must shift more to the right as they get further from end mirror to balance the increased wavevector

Phasors of the light field

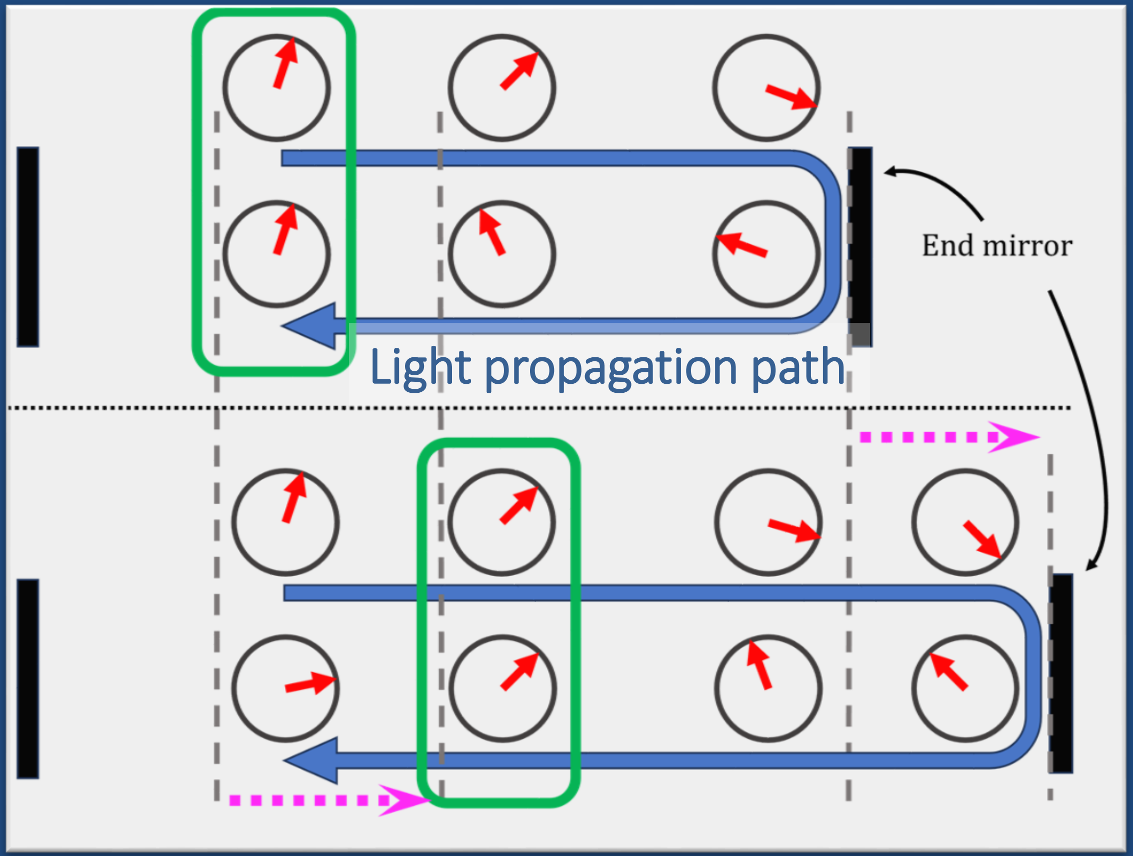

arXiv:2603.07302

Input/End-mirror asymmetry and consequences

- Antinodes appear where counterpropagating waves are in phase
- Phase offset is simple for end mirror reflection
    - In slow motion limit, end mirror is the exact midpoint → antinodes anchored to end mirror
- Multiple key consequences when $\Omega \ll \kappa$:
    - Input mirror motion does not displace antinodes
        - Displacement noise highly suppressed
    - Common mode motion *does* couple significantly

Phasors of the light field

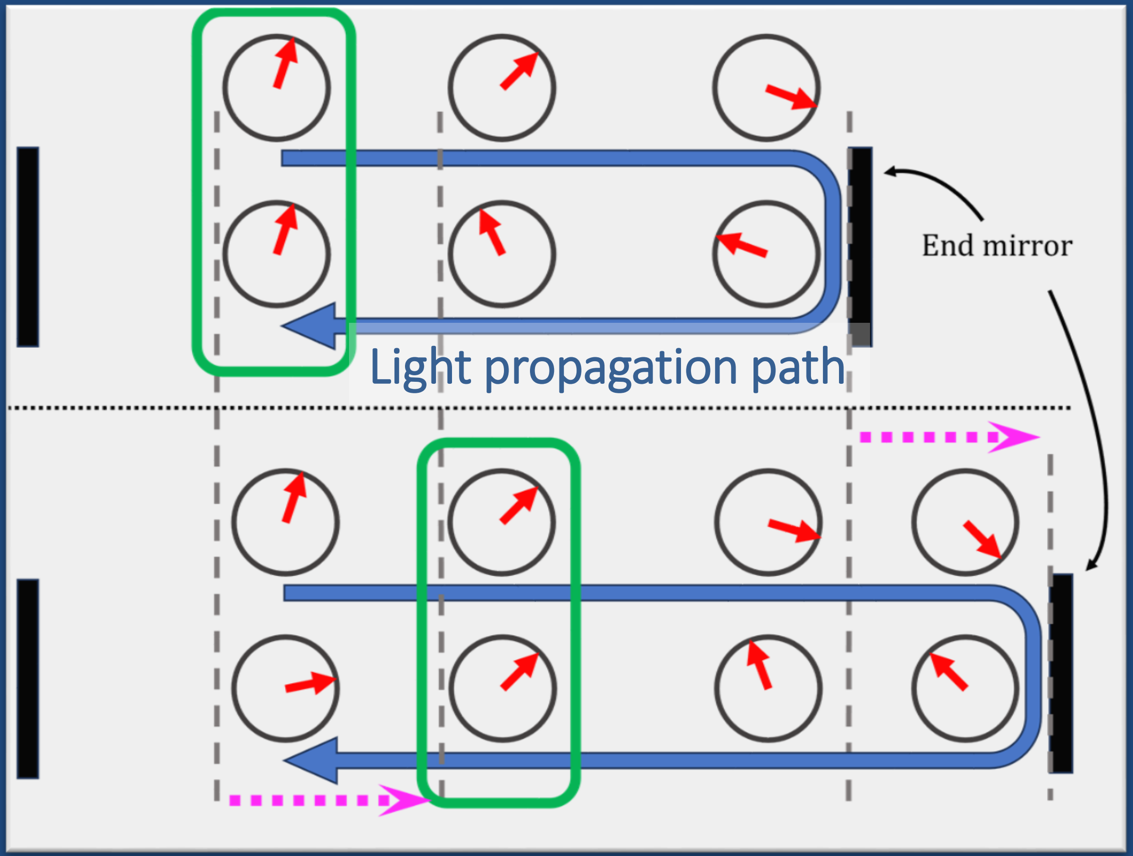

arXiv:2603.07302

Relativistic antinode-sensor displacement at high Ω

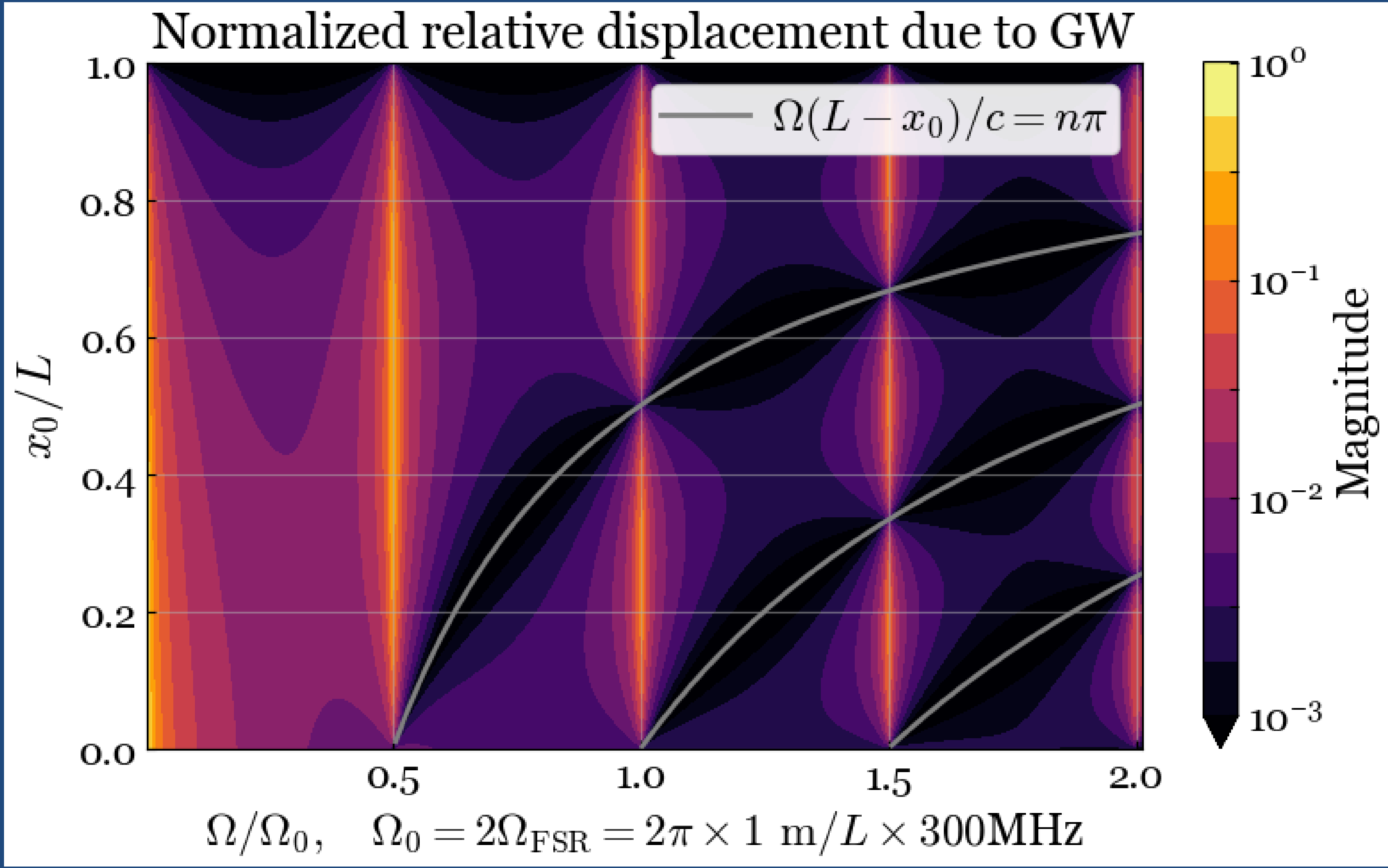

Relativistic antinode-sensor displacement at high Ω

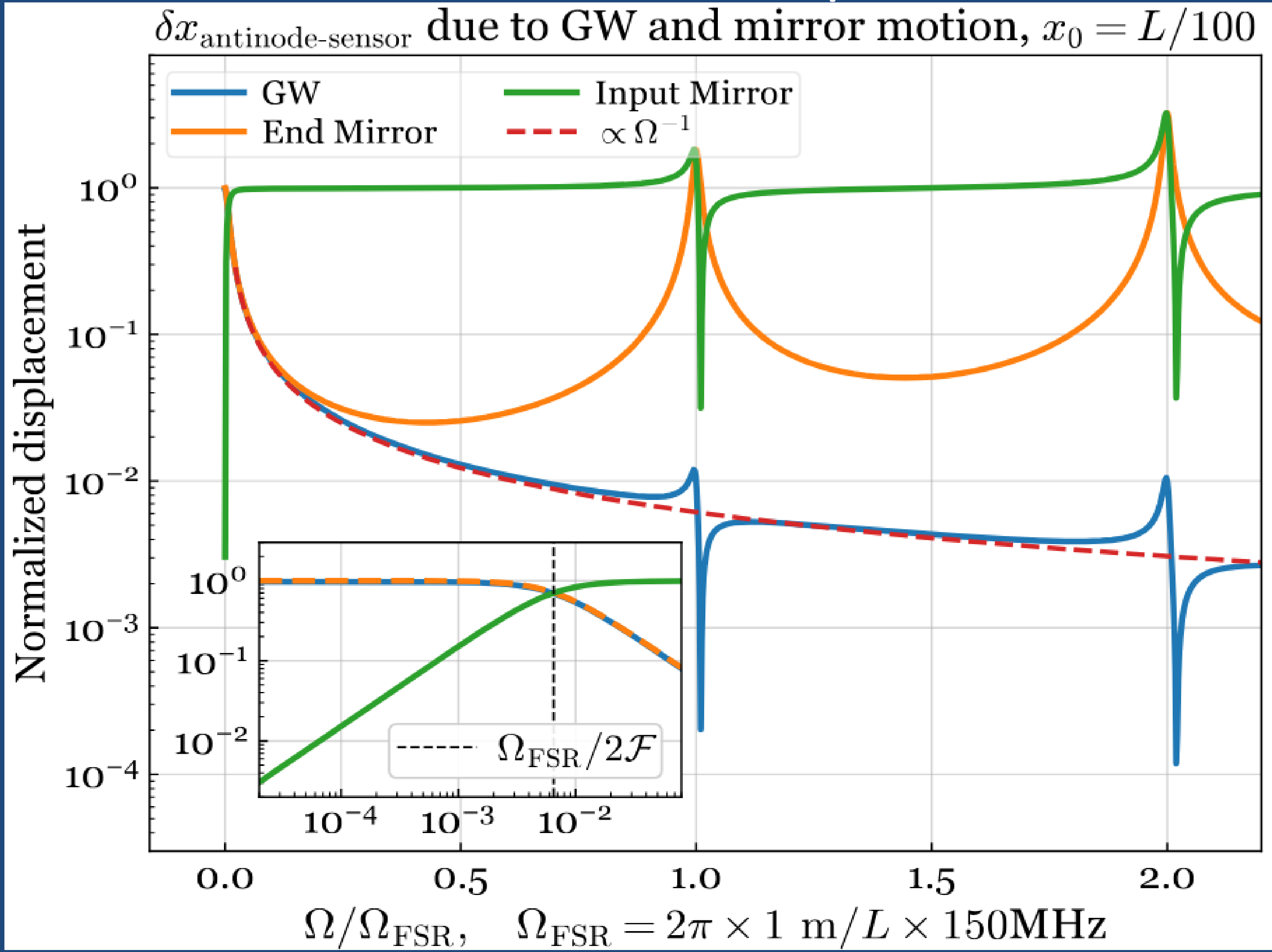

Moving beyond the small particle limit

- What if the levitated sensor is large enough to affect the global cavity fields?
  - Plate-like sensors have been proposed for more efficient detection

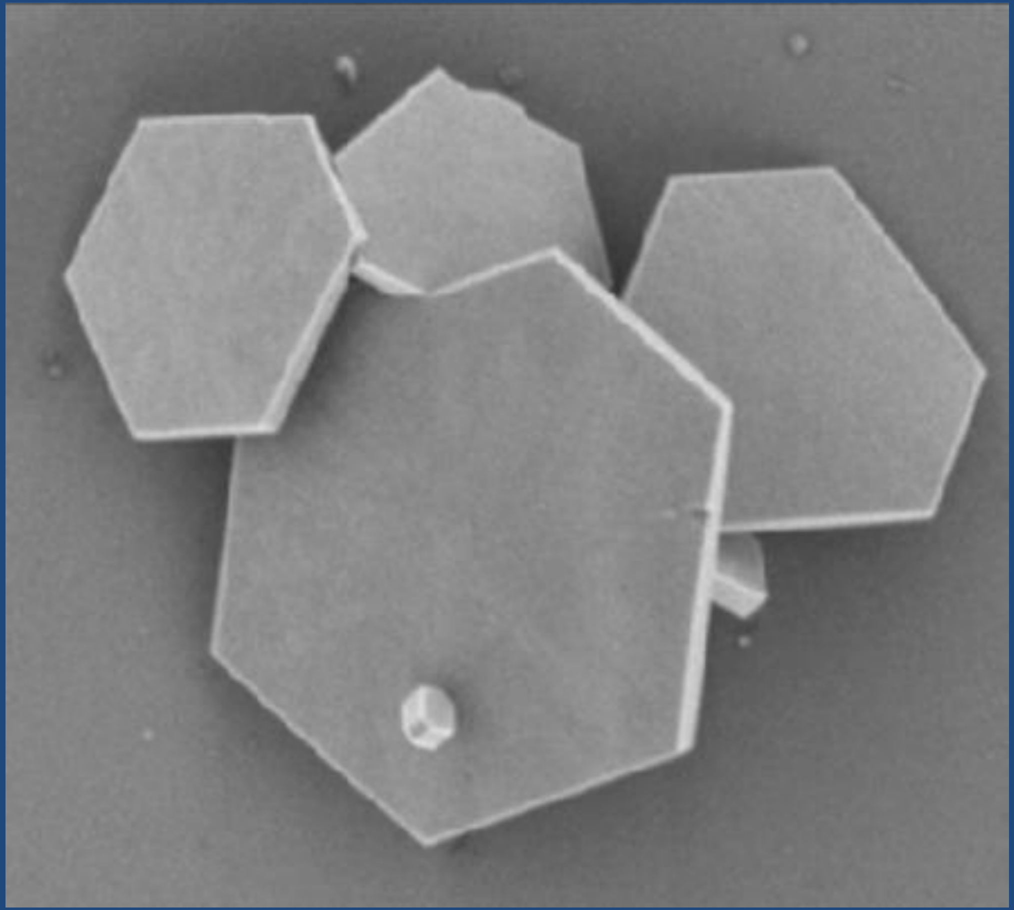

arXiv:2204.10843

Moving beyond the small particle limit

- What if the levitated sensor is large enough to affect the global cavity fields?
  - Plate-like sensors have been proposed for more efficient detection
- Aim to compute full field solutions rather than standard perturbative methods

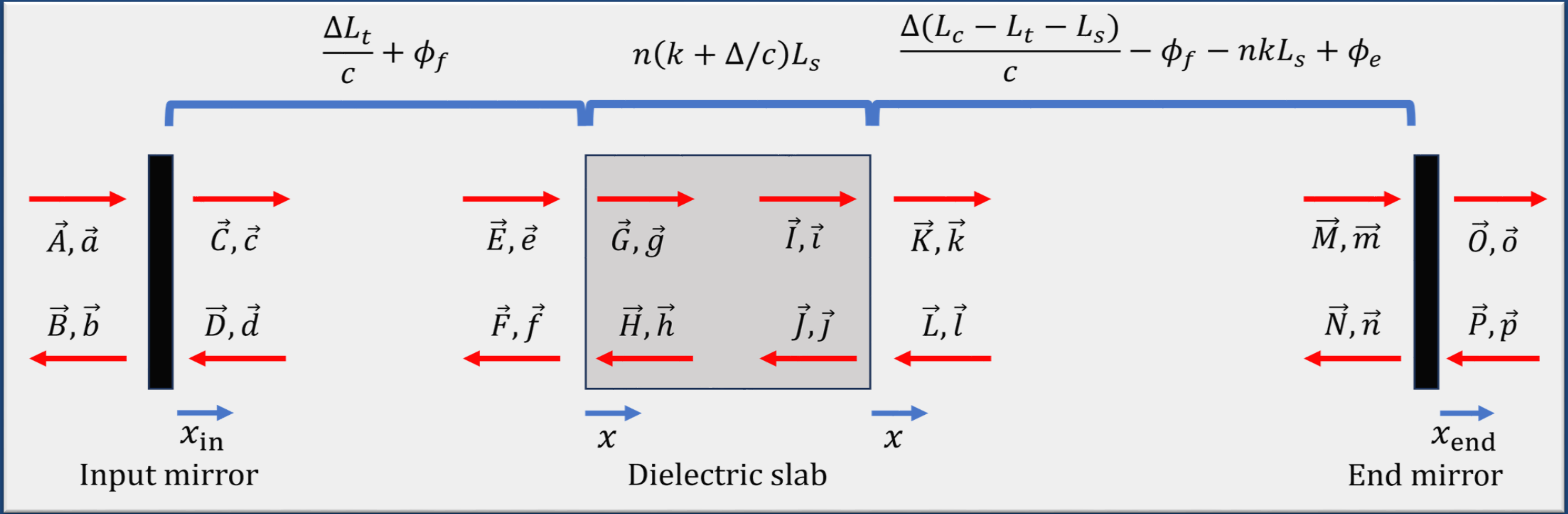

Moving beyond the small particle limit

- What if the levitated sensor is large enough to affect the global cavity fields?
  - Plate-like sensors have been proposed for more efficient detection
- Aim to compute full field solutions rather than standard perturbative methods
- Operating in between the levitated particle / membrane spaces requires careful calculation of optical forces

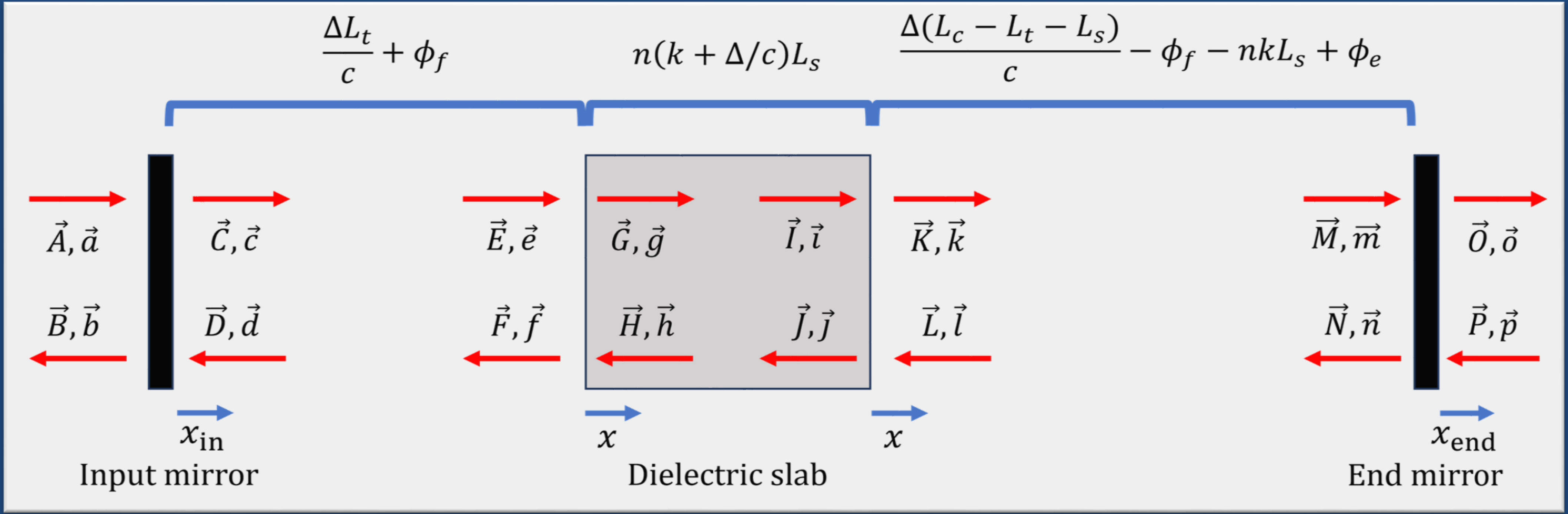

Moving beyond the small particle limit

- What if the levitated sensor is large enough to affect the global cavity fields?
  - Plate-like sensors have been proposed for more efficient detection
- Aim to compute full field solutions rather than standard perturbative methods
- Operating in between the levitated particle / membrane spaces requires careful calculation of optical forces
- Forthcoming paper on transfer function calculation in the two-photon formalism

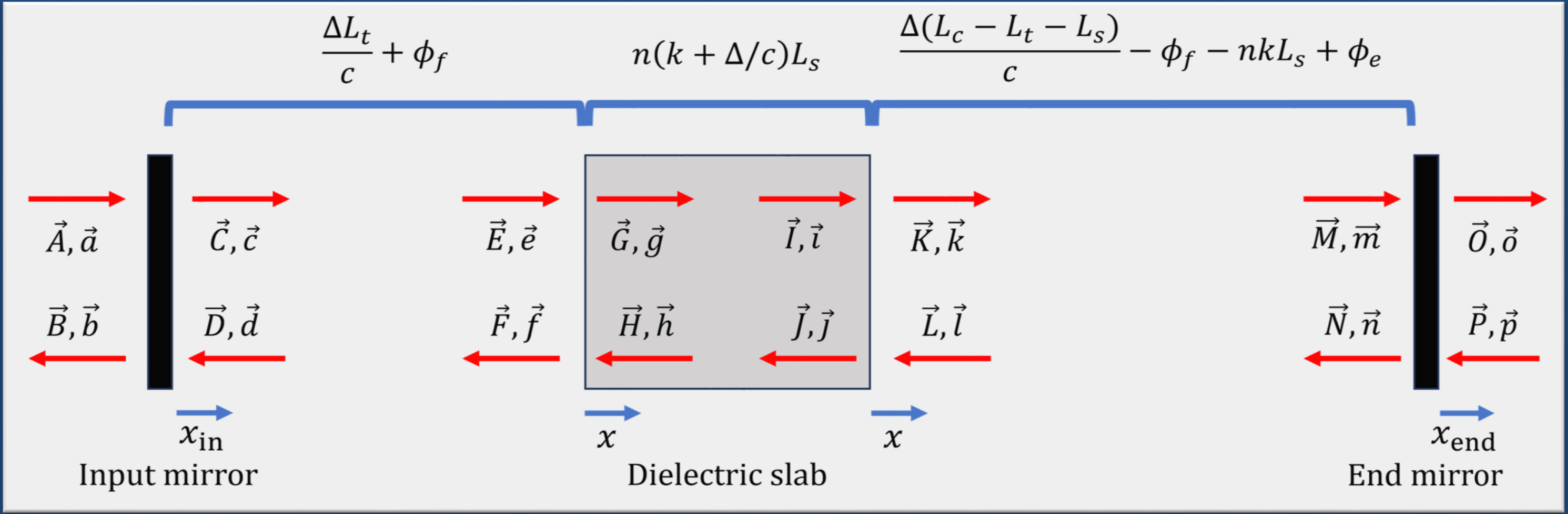

Cavity splitting due to thin plate-like dielectrics

- Inserting the dielectric plane into cavity heavily modifies internal fields
  - Position-dependent split Lorentzian

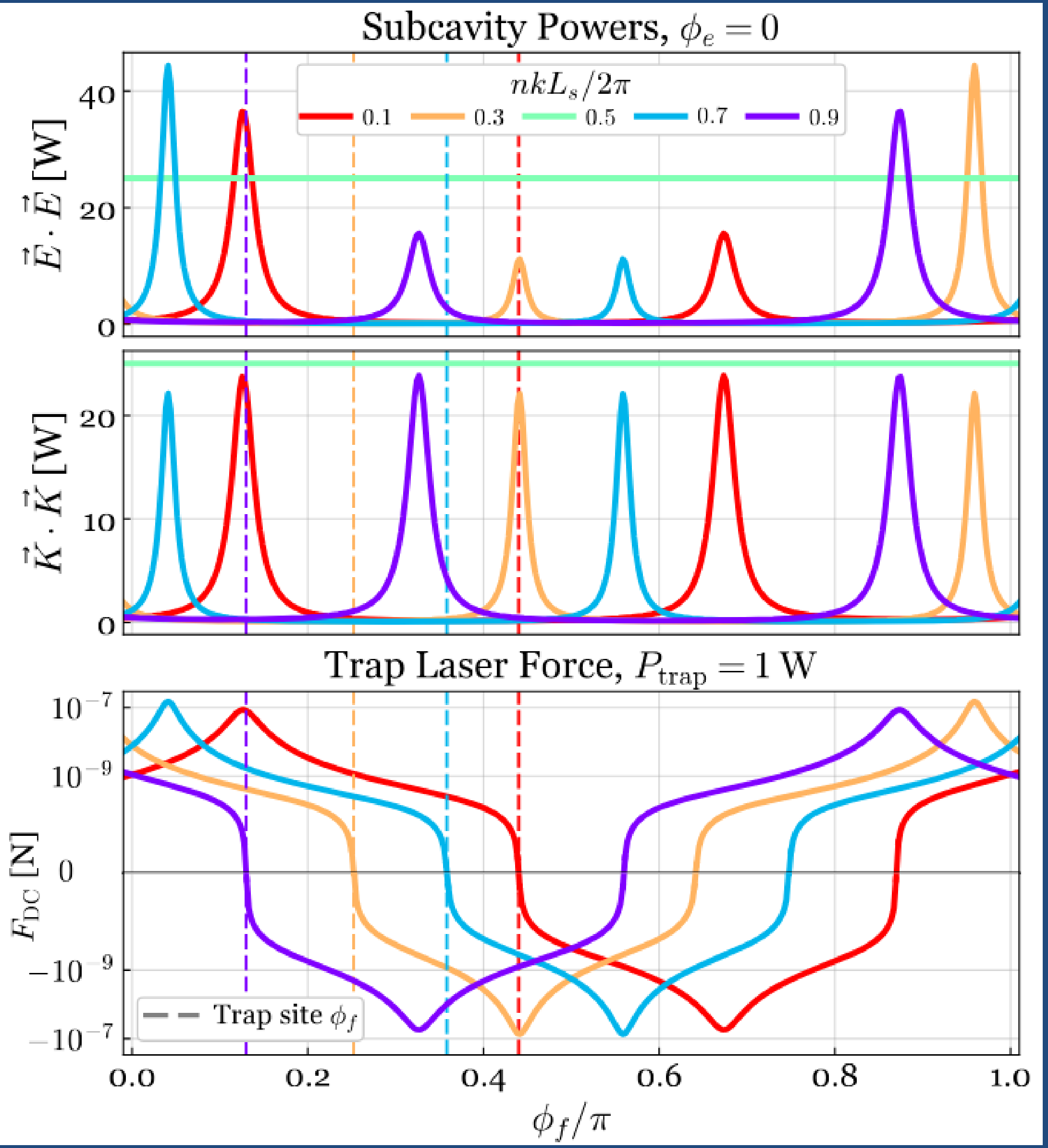

Cavity splitting due to thin plate-like dielectrics

- Inserting the dielectric plane into cavity heavily modifies internal fields
  - Position-dependent split Lorentzian
- Dielectric has effectively split system into two subcavities which can each resonate

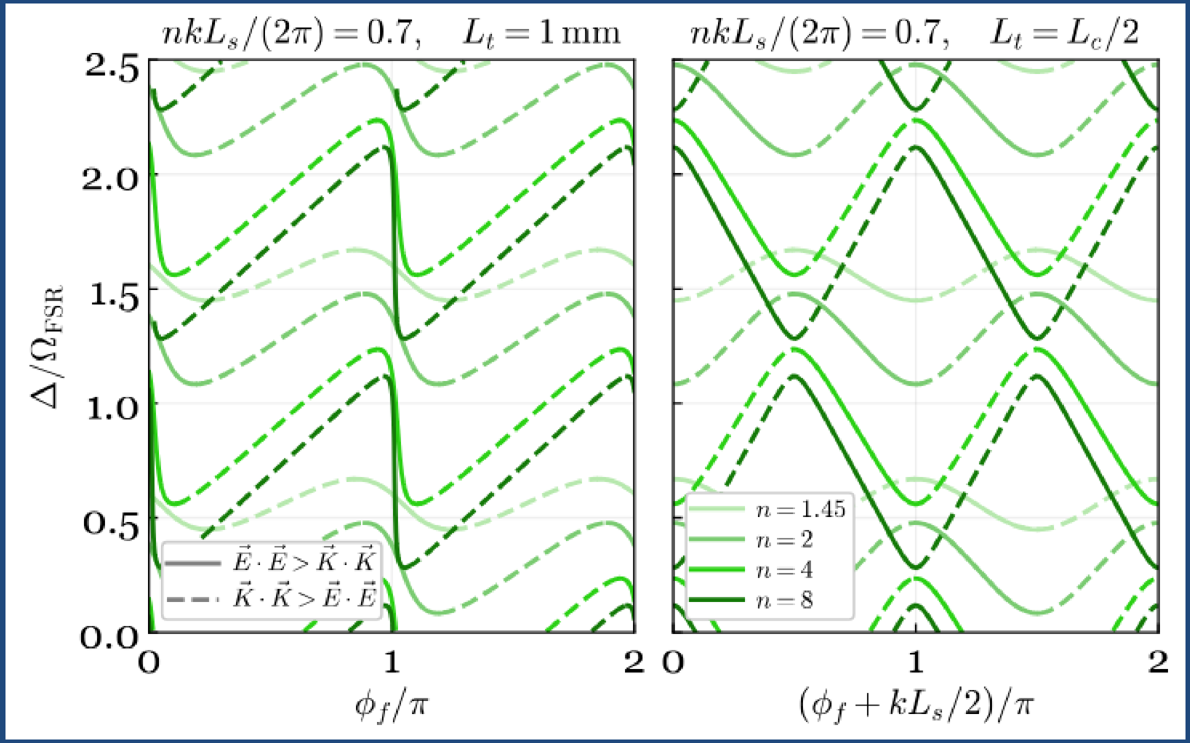

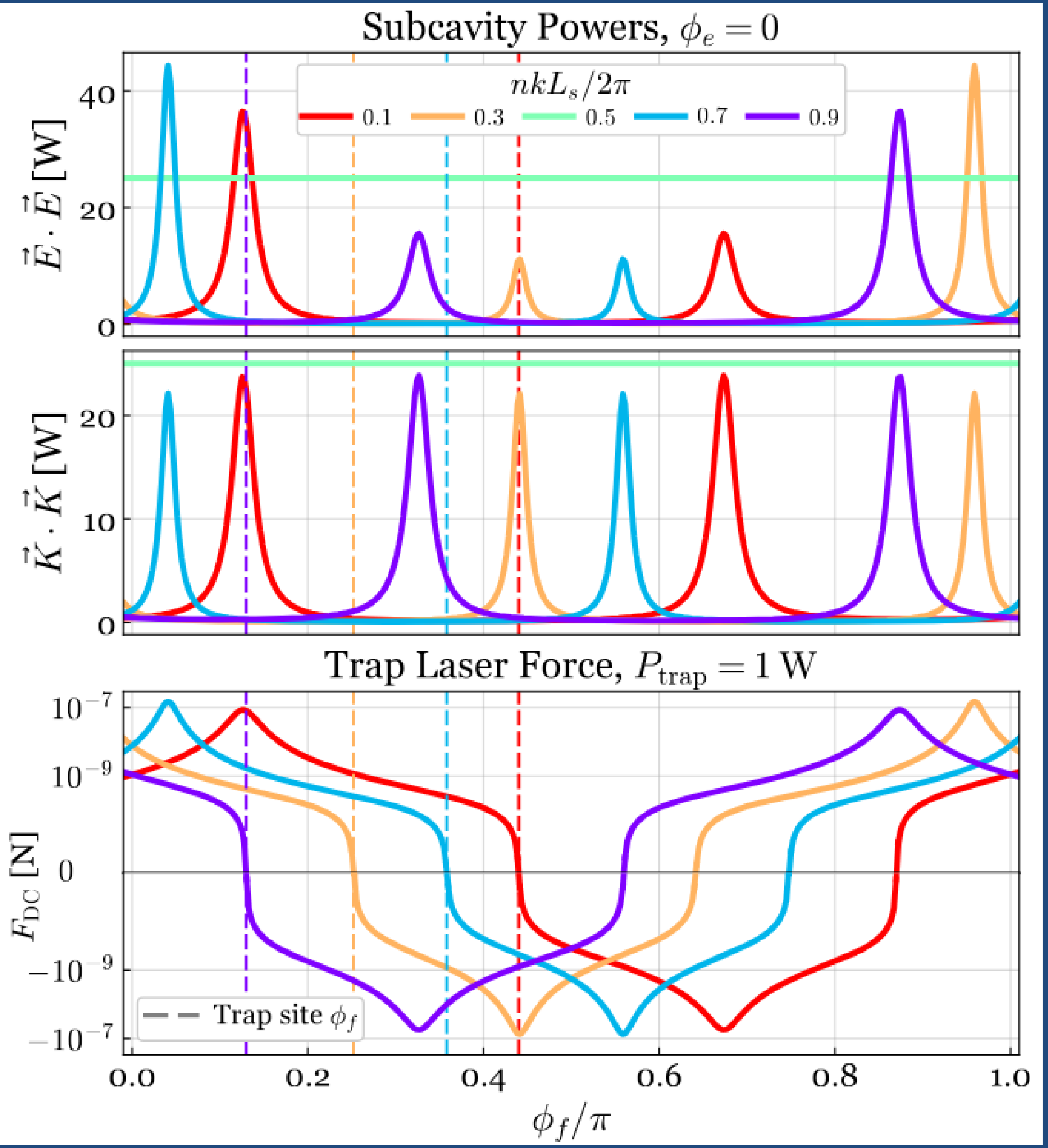

Cavity splitting due to thin plate-like dielectrics

- Inserting the dielectric plane into cavity heavily modifies internal fields
  - Position-dependent split Lorentzian
- Dielectric has effectively split system into two subcavities which can each resonate

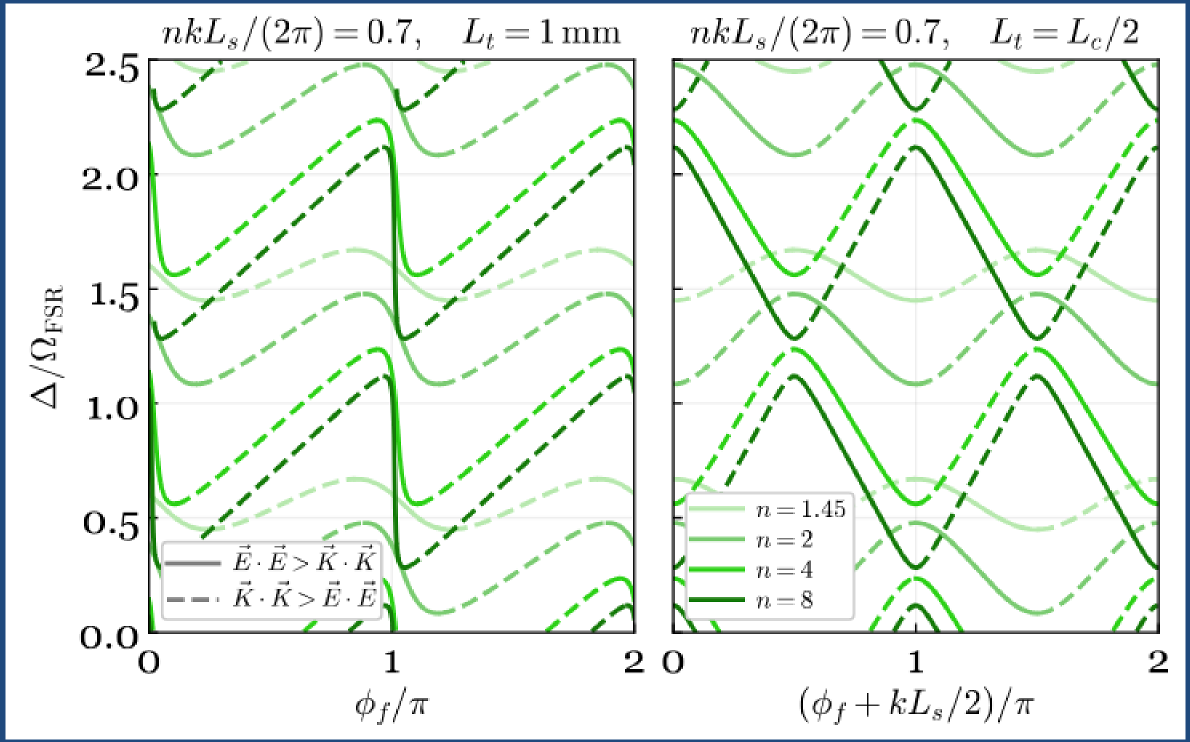

A thin membrane-in-the-middle:

- Internal non-vacuum propagation gives vertical shifts

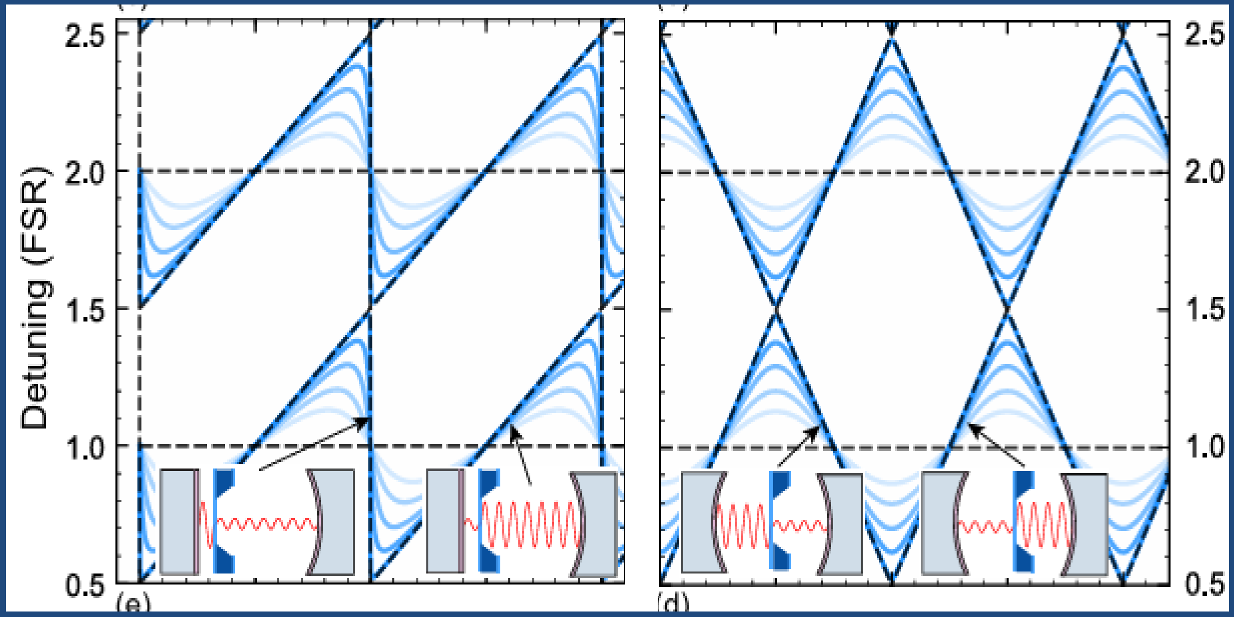

Dumont, V., et al. *Flexure-Tuned Membrane-at-the-Edge Optomechanical System* (2019).

Further shortcomings of perturbation theory

- Optomechanical coupling computed perturbatively: $\delta\omega_c \approx \frac{\int d^3\vec{x}\;\delta\epsilon(\vec{x})\vec{E}_0^2(\vec{x})}{\int d^3\vec{x}\;\vec{E}_0^2(\vec{x})}$, $g_0 \equiv \frac{\partial\omega_c}{\partial x}$

Further shortcomings of perturbation theory

- Optomechanical coupling computed perturbatively: $\delta\omega_c \approx \frac{\int d^3\vec{x}\,\delta\epsilon(\vec{x})\vec{E}_0^2(\vec{x})}{\int d^3\vec{x}\,\vec{E}_0^2(\vec{x})}$, $g_0 \equiv \frac{\partial\omega_c}{\partial x}$
- This approximation scheme breaks down even at $\sim \lambda/10n$

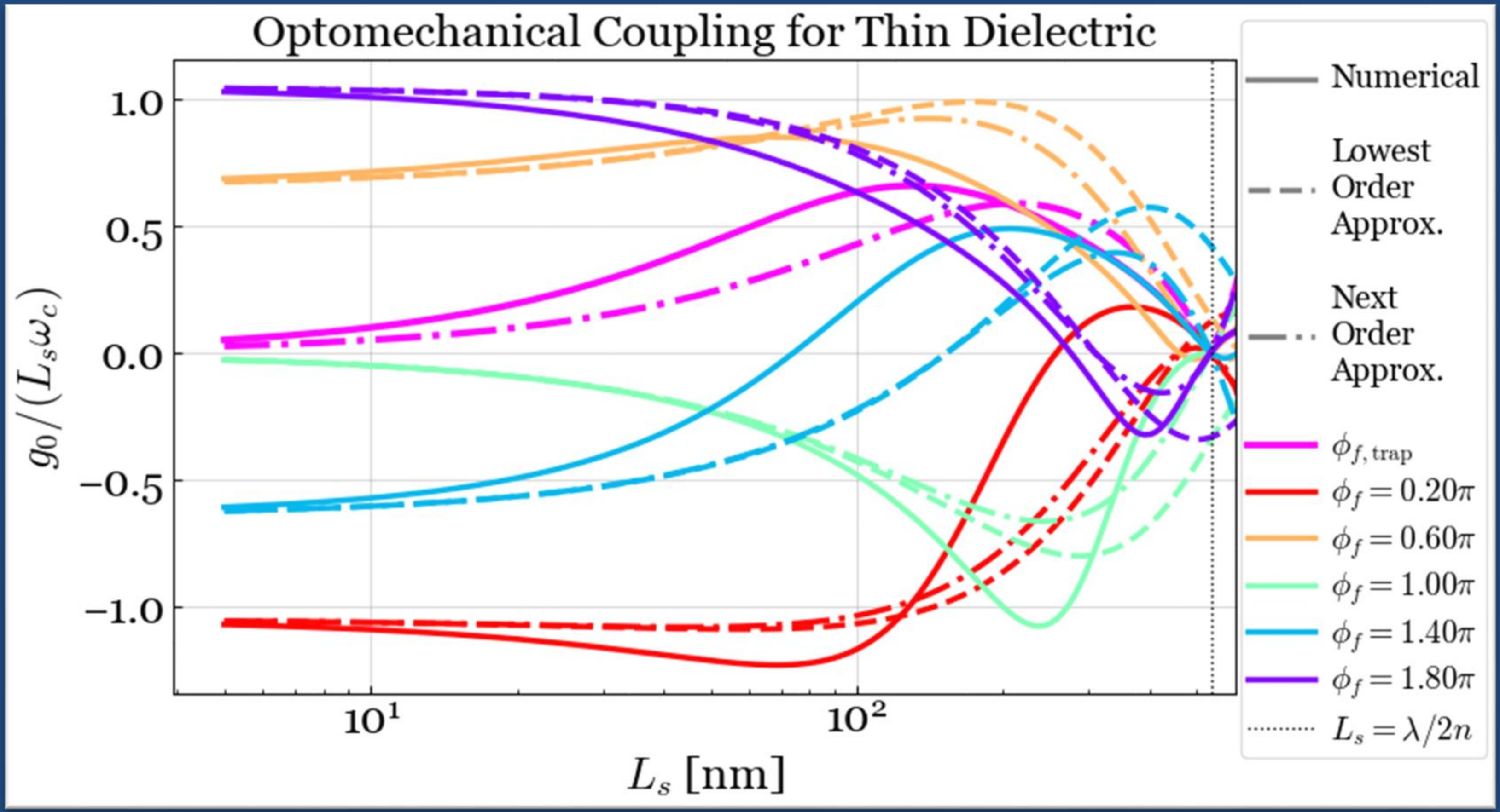

Conclusions

- Levitated sensors appear to be a promising avenue for high-frequency GW detection
- We are closing gaps in our knowledge of how to design and operate such detectors
- A careful derivation of the gauge-invariant trap site offset due to a GW clarifies the origin of a non-intuitive, yet exploitable, asymmetry in the result
- It also reveals phenomena at higher frequencies which must be accounted for in designs of future iterations of these experiments

alaeuger@caltech.edu

Conclusions

- Levitated sensors appear to be a promising avenue for high-frequency GW detection
- We are closing gaps in our knowledge of how to design and operate such detectors
- A careful derivation of the gauge-invariant trap site offset due to a GW clarifies the origin of a non-intuitive, yet exploitable, asymmetry in the result
- It also reveals phenomena at higher frequencies which must be accounted for in designs of future iterations of these experiments
- When the sensor is large and captures entire beam cross-section, a new procedure for computing full field response to incident perturbations is needed
- We demonstrated this system can easily violate perturbative expectations used to analyze more typical levitated sensor experiments

alaeuger@caltech.edu

Additional Slides

Cavity splitting due to thin plate-like dielectrics

- Inserting the dielectric plane into cavity heavily modifies internal fields
  - Position-dependent split Lorentzian
- Dielectric has effectively split system into two subcavities which can each resonate
- Sensor equilibrium position lies in between the split peaks → low spring constant

- What if we allow for cavity locking?
  - Basic model: lock to max P_{trans}
- Split Lorentzians nearly converge, trap site can lie where subcavity powers are high
  - Trap frequencies should be magnified

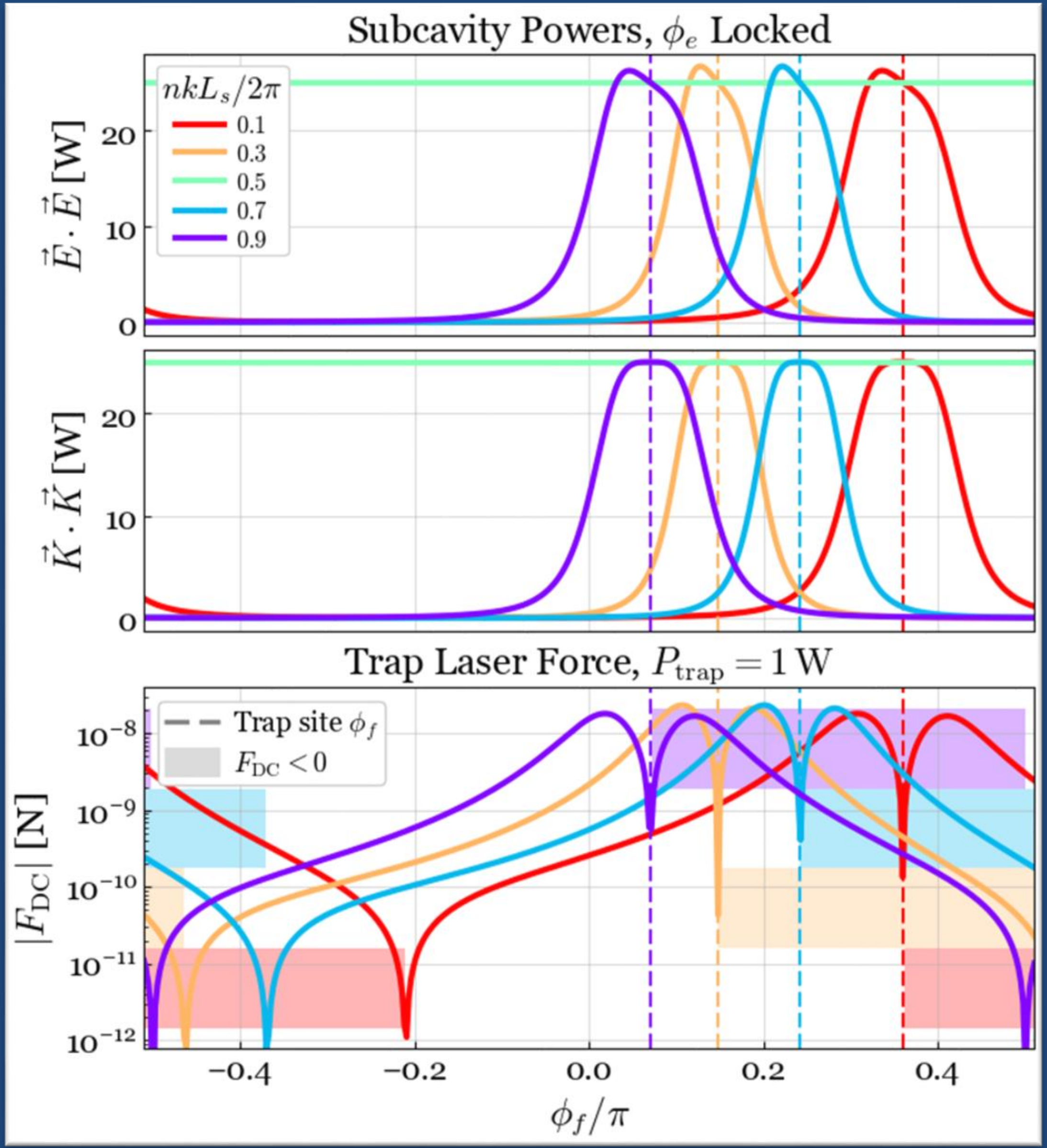

Cavity splitting due to thin plate-like dielectrics

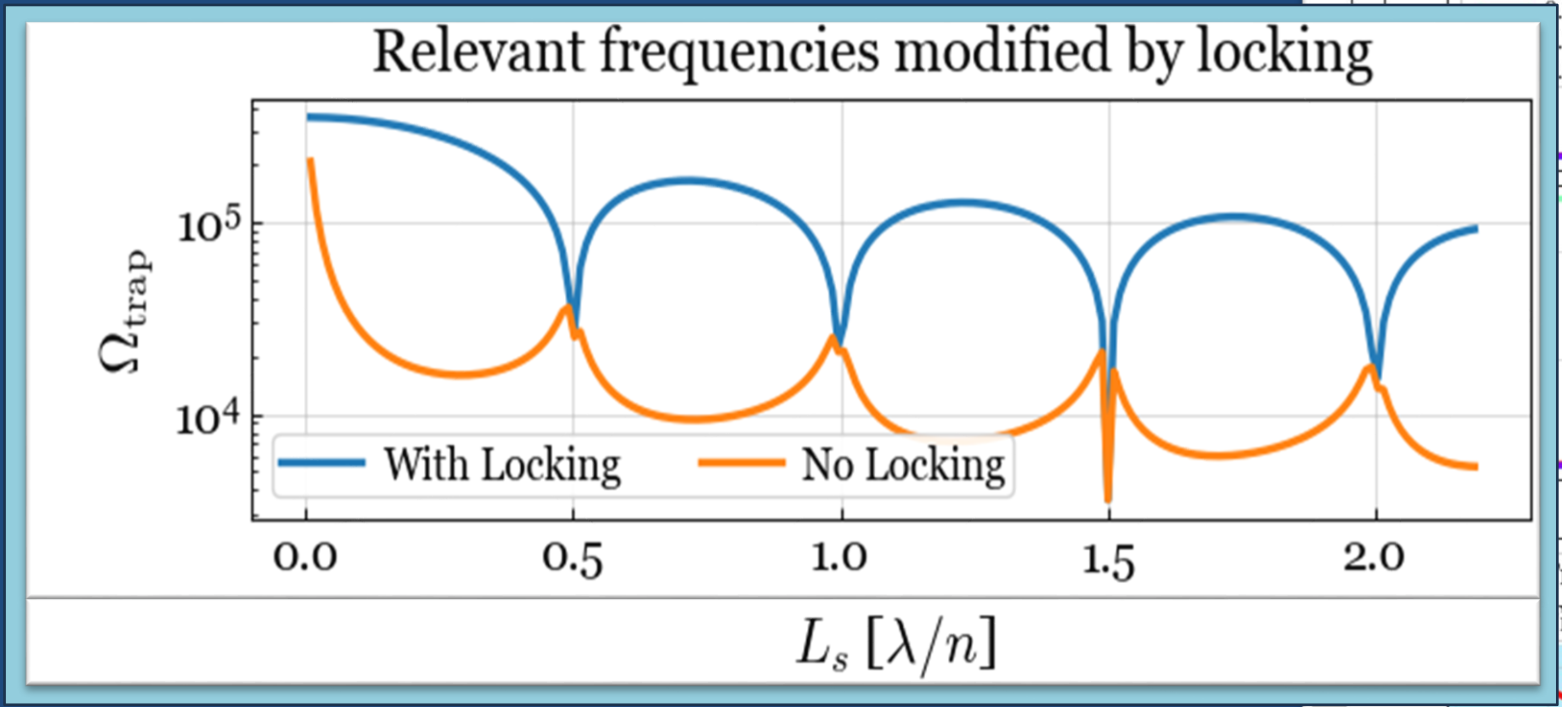

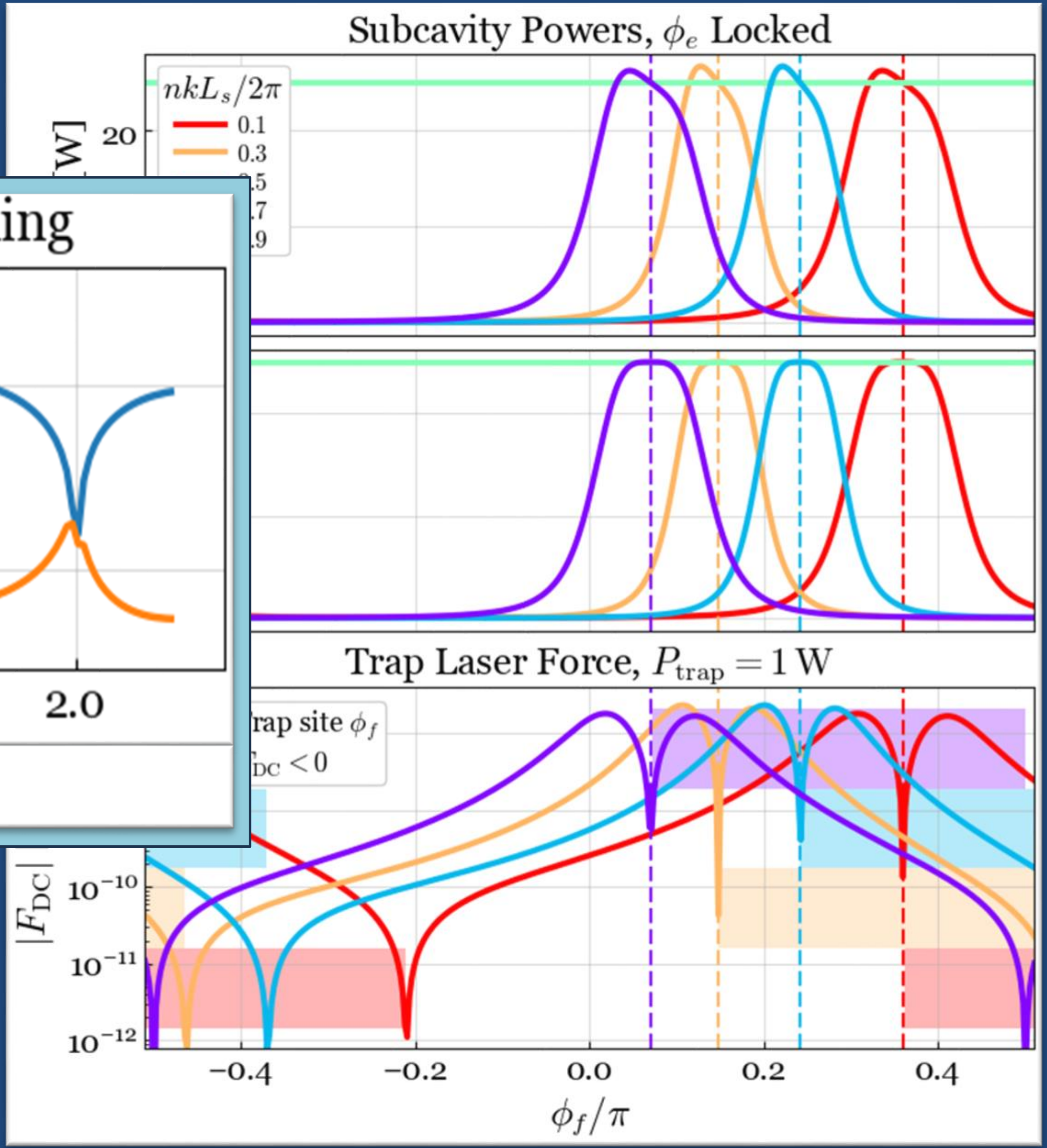

Transfer functions from GW and noise ports

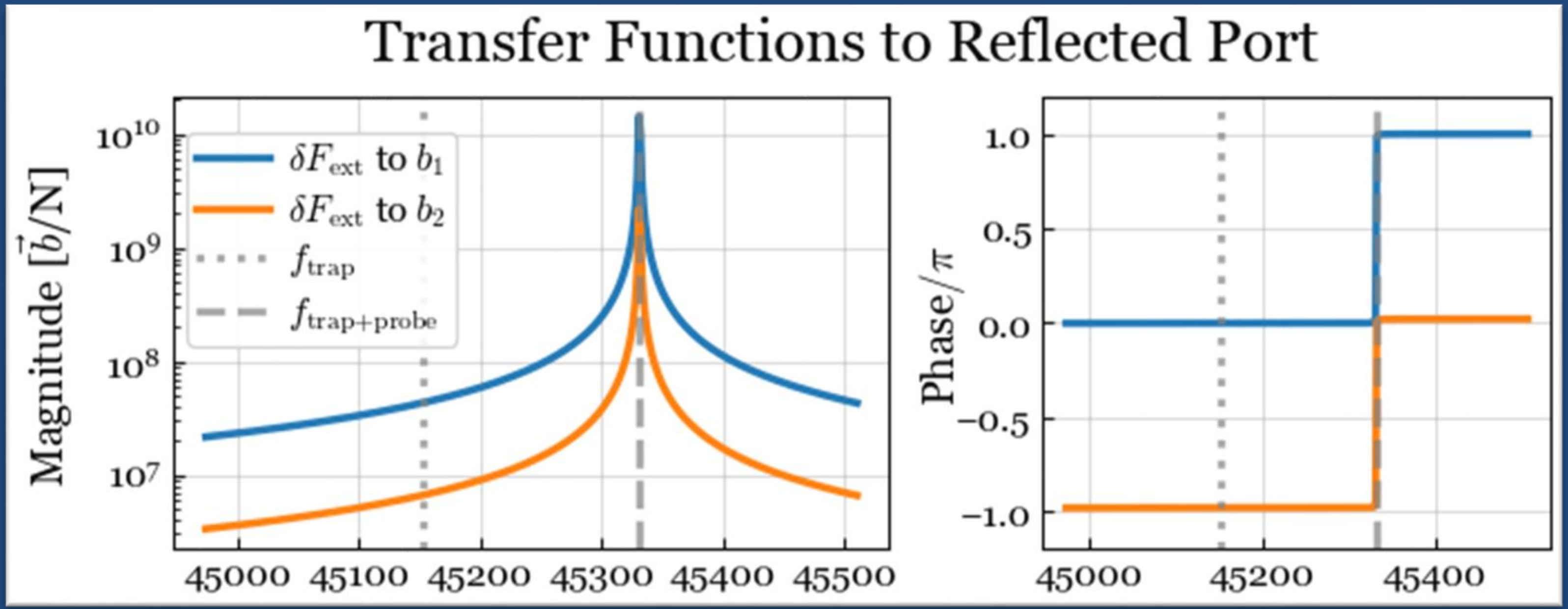

- Force transfer functions peak at the cooled resonant frequency
- Hierarchy in coupling to b_1 and b_2 dictated by detuning

Transfer functions from GW and noise ports

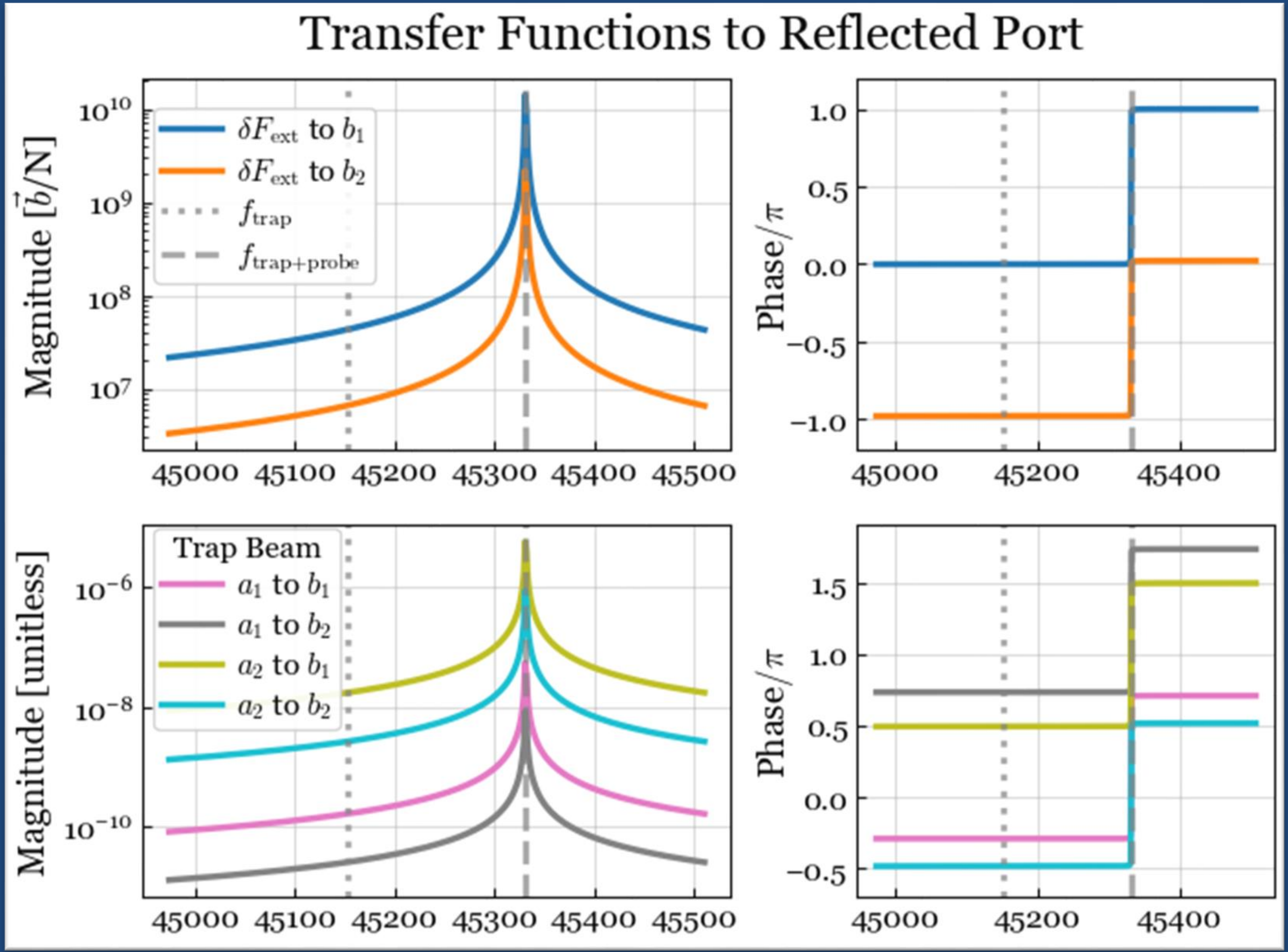

- Force transfer functions peak at the cooled resonant frequency
- Hierarchy in coupling to b_1 and b_2 dictated by detuning
- Trap beam fluctuation transfer functions couple primarily through force on sensor

Transfer functions from GW and noise ports

- Mirror displacement transfer functions feature a direct and indirect component

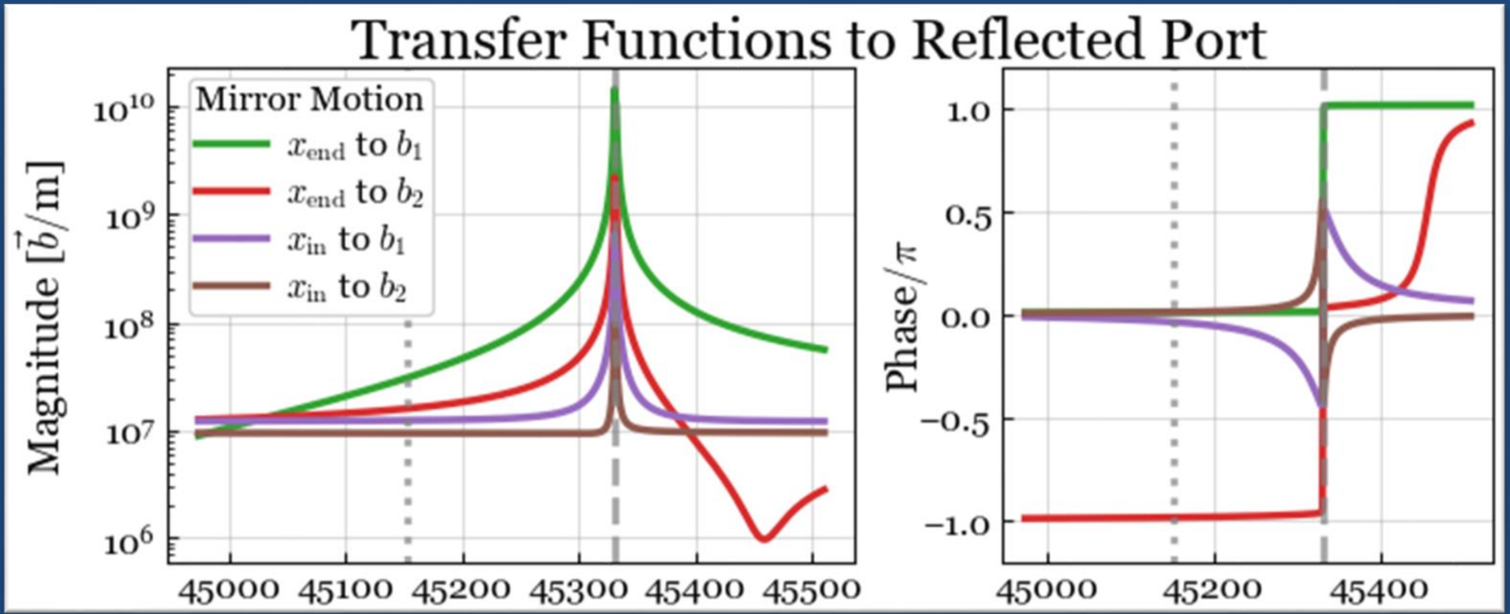

Transfer functions from GW and noise ports

- Mirror displacement transfer functions feature a direct and indirect component
- We can compute effective trap site displacement due to mirror motion by normalizing by force TF
- Even with the cavity split into subcavities, the low frequency results of relativistic calculation hold!